Possible Evidences for existence of an Aether Medium (or Virtual Inertia/Spin Superfluid Medium)

Outline of presentation by V. Christianto* & Florentin Smarandache**[1]

*Malang Institute of Agriculture, East Java, Indonesia

**Dept. Mathematics and Sciences, University of New Mexico, Gallup, NM, USA

Introduction:

The present article explores the possibility of an aether medium, also referred to as a virtual inertia/spin superfluid medium, existing to explain certain physical phenomena. While the concept of an aether has been historically rejected by mainstream physics, recent findings and interpretations offer potential justifications for its reconsideration. After discussions with several physicists, notably Robert N. Boyd, PhD and others, we are convinced that aether medium does exist, or may be called virtual inertia/spin superfluid medium.

Here, we will delve into three evidence-based models suggesting the existence of such a medium:

1.**Refutation of Planck's Constant by Cameron Rebigsol:** Rebigsol's work challenges the fundamental constant of Planck's constant, suggesting its dependence on the Earth's motion through the aether. This implies that the constant might not be truly universal, hinting at the presence of an underlying medium influencing physical processes.

2.**Aspden's Virtual Inertia:** This model proposes a form of inertia inherent to the vacuum itself, arising from the interaction of virtual particles. This "virtual inertia" could explain various physical phenomena, potentially aligning with the concept of an aether as a medium with inherent properties.

3.**Huygens's Pendulum Synchronization and the Kuramoto Model:** The classic experiment of synchronized pendulums by Huygens has been explained by the Kuramoto model, which requires an interaction medium between the pendulums. This could be interpreted as evidence for an aether-like medium facilitating the synchronization.

Each of these models presents intriguing challenges to the current understanding of physics. While alternative explanations and interpretations exist, they cannot be definitively ruled out at this stage. Further research and experimentation are crucial to validate or refute these models and their implications for the existence of an aether medium.

[1] With assistance of bard.google.com

Discussions:

A. Aspden's Virtual Inertia: A Stepping Stone Towards an Aether Superfluid?

The notion of an aether, a mysterious medium permeating all of space, has captivated physicists for centuries. Despite its historical rejection, recent discoveries like Dr. Harold Aspden's virtual inertia continue to spark debate and offer intriguing hints towards its potential existence. This article delves into Aspden's groundbreaking work and explores how it might pave the way for understanding a superfluid aether medium.

Virtual Inertia: A Paradigm Shift?

Aspden's virtual inertia theory proposes a fascinating twist on our understanding of inertia. He suggests that the vacuum itself possesses a form of inertia, arising from the dynamic interactions of virtual particles constantly popping in and out of existence. This "virtual inertia" exhibits properties akin to mass and momentum, even in the absence of any physical matter.

Intriguing Parallels with the Aether:

The concept of virtual inertia bears striking similarities to the classical notion of an aether. Both propose a medium permeating all of space, influencing physical phenomena without directly interacting with matter. While the aether was historically envisioned as a material substance, virtual inertia suggests a more nuanced interaction, mediated by the quantum vacuum's inherent properties.

Potential Implications for an Aether Superfluid:

Superfluids are exotic states of matter characterized by zero viscosity, allowing them to flow effortlessly. If the virtual inertia arises from a dynamic interplay of virtual particles, it could be interpreted as a superfluid-like aether. This aether wouldn't be a stationary substance but rather a constantly fluctuating sea of virtual activity, influencing physical processes through its inherent properties.

Challenges and Future Directions:

While Aspden's work is groundbreaking, it's important to acknowledge the challenges it faces. The exact nature of virtual inertia and its connection to gravity and other fundamental forces remain open questions. Further theoretical and experimental work is crucial to validate the theory and explore its implications for an aether superfluid.

B. Synchronization between two pendulums: Unmasking the Dance with an Aether?

From the elegant halls of science museums to the rhythmic sway of metronomes, the synchronized swing of two pendulums has mesmerized minds for centuries. This captivating phenomenon, first observed by Christiaan Huygens in the 17th century, has continued to intrigue physicists, finding

new interpretations and explanations throughout history. Today, we delve into the secrets of this dance, exploring the intricate connection between synchronization, the Kuramoto model, and the possibility of an underlying aether medium.

The Pendulum's Tale: From Observation to Explanation

Huygens's initial observation ignited a wave of research, seeking to understand the unseen forces guiding the pendulums' harmonious movement. In 1983, Steven Strogatz, in his renowned book "Sync," brought light to the phenomenon through the Kuramoto model. This mathematical framework elegantly explained how seemingly independent pendulums, under weak coupling, can entrain their swings to achieve mesmerizing synchrony. However, the nature of this coupling remained somewhat elusive.

Enter the Intriguing Stage: Can an Aether Play a Role?

While the Kuramoto model provides a powerful theoretical framework, some intriguing questions linger. Does this coupling necessitate a physical medium for interaction? This is where the concept of an aether, a hypothetical universal medium, enters the stage. By proposing the existence of an aether, we could postulate that it acts as a mediator, carrying the subtle influences that nudge the pendulums towards synchrony.

C. A Proposed Experiment

To explore this possibility, let's envision a modified experiment. Introduce a thin metal plate between the swinging pendulums. If an aether truly exists, its interaction with the plate could alter the synchronization dynamics. According to the proposed aether model, the plate might dampen or amplify the coupling between the pendulums, affecting their synchronization time or final state. Conversely, if no aether exists, the presence of the plate should have minimal impact on the synchronization observed through the Kuramoto model.

The Weight of Evidence: Unveiling the Truth

The outcome of this proposed experiment would hold significant weight. If the synchronization behavior deviates from the predictions of the unperturbed Kuramoto model, it could lend credence to the existence of an aether influencing the interaction. However, it's crucial to remember that alternative explanations might also exist, requiring further investigation and potentially more complex experimental designs.

Beyond the Pendulums: Implications and Open Questions

While the pendulum experiment offers an intriguing starting point, the implications of an aether extend far beyond this specific phenomenon. Its existence could impact our understanding of various physical interactions, from gravity to electromagnetism. However, numerous questions remain unanswered. What are the properties of this aether? How does it interact with matter and

other fundamental forces?

A bit discussion of Kuramoto model (while it is not yet including an effect of physical aether medium)[2]

The Kuramoto model is typically used to describe the synchronization of coupled oscillators. It doesn't explicitly involve the concept of a physical ether medium. Assuming a standard Kuramoto model, where the dynamics of a set of coupled oscillators are described by a system of differential equations, here's a general example in Mathematica.

```
(* Define the Kuramoto model parameters *)

n = 2; (* Number of oscillators *)

couplingStrength = 0.1; (* Coupling strength *)



(* Define the Kuramoto model equations *)

kuramotoEquations = Table[

  θ'[t, i] == ω[i] + couplingStrength Sum[Sin[θ[t, j] - θ[t, i]], {j, 1, n}] / n,

  {i, 1, n}

];



(* Initial conditions *)

initialConditions = Table[θ[0, i] == RandomReal[{0, 2 π}], {i, 1, n}];



(* Solve the differential equations *)
```

[2] Written by assistance by http://chat.openAI.com

```
solution = NDSolve[{kuramotoEquations, initialConditions}, Table[θ[t, i], {i, 1, n}], {t, 0, 10}];


(* Plot the solutions *)

Plot[Evaluate[Table[θ[t, i] /. solution, {i, 1, n}]], {t, 0, 10},

  PlotLegends -> Table["Pendulum " <> ToString[i], {i, 1, n}],

  FrameLabel -> {"Time", "Angle"},

  PlotLabel -> "Kuramoto Model for Synchronization"]
```

Conclusion: A Symphony Unfinished

The synchronization of pendulums serves as a captivating case study, reminding us that seemingly simple phenomena can harbor profound mysteries. While the proposed experiment presents an opportunity to explore the potential role of an aether, it's merely the first note in a larger symphony of discovery. The quest to understand the hidden forces governing our universe continues, and the pendulum's swing invites us to join the dance, ever curious and ever seeking the truth beyond the visible.

D. Illustrations of Proposed experiment set

Illustration 1. Synchronization between two pendulums interfered by amplified laser pen

Illustration 2. Synchronization between two pendulums, interfered with thin metal plate located in-between


Illustration 3. Synchronization between two pendulums, interfered with a beryl crystal located in-between

Key Points:

- The article acknowledges the historical rejection of aether but presents recent findings as potential justifications for its reconsideration.
- Three evidence-based models are outlined: Rebigsol's Planck's constant refutation, Aspden's virtual inertia, and Huygens's pendulum synchronization.
- The article emphasizes the need for further research and experimentation to validate or refute these models and their implications.

Concluding remark

Aspden's discovery of virtual inertia throws open exciting new avenues for exploring the nature of space and the possibility of an aether medium. While the path towards definitive proof remains long, his work serves as a stepping stone, urging us to reconsider our understanding of the vacuum and its potential role in shaping physical phenomena. As we delve deeper into the mysteries of the quantum world, the possibility of an aether superfluid might not be as fantastical as it once seemed.

Other than that, the synchronization of pendulums serves as a captivating case study, reminding us that seemingly simple phenomena can harbor profound mysteries. While the proposed experiment presents an opportunity to explore the potential role of an aether, it's merely the first note in a larger symphony of discovery. The quest to understand the hidden forces governing our universe continues, and the pendulum's swing invites us to join the dance, ever curious and ever seeking the truth beyond the visible.

We also outlined here a number of possible experiments with two pendulums to prove that spin superfluid medium is necessary to mediate the effect of synchronization, including interfering the space between two-pendulums with amplified laser exposure (to disturb the aether), or with thin metal plate, or with beryl crystal.

Version 1.0: 3rd feb 2024, pk. 17:25

VC, FS

Appendix:
- Rebigsol’s article

- article on Kuramoto model

The Third Evidence of Aether

— Photoelectric Effect and the Classical Physics Endorse Each Other Back to Back—

2020 © *Cameron Rebigsol*

Abstract It has been for more than a century that in the modern physics campus classical physics is chided as being incapable of proposing convincing explanation on the photoelectric effect. However, to this author, there appears some interesting evidence that witnesses the opposite. As the number one evidence, Fig.01 in the text portion of this article shows many curves defying the linearity supposedly entitled on them by the equation $E_{max} = hf - W$, which is proposed based on the concept of photon, or quantum in explaining the photoelectric effect. Contrary to the chiding from the modern physics, as we will see, classical physics, relying on the assumption of existence of Aether, can explain the geometry behavior of all these curves, while exposing the self-refutation nature of the equation $E_{max} = hf - W$. This author believe that classical physics has shown us an abundance of credits for it to reclaim its authority in the study of physics. If we ever apply it and found it fails us, do not blame classical physics, but reexamine our work!

Keywords Relativity, photon, quantum, Aether, photoelectron, anode, cathode

Contents

1. The Five Arguments

Argument One *Einstein's renowned photoelectric equation is challenged by experiment data.*

So far, the theory behind Eq. 01 below, proposed by Einstein, is the most prevalent theory in modern physics in explaining the photoelectric phenomenon

$$K_{max} = hf - W \qquad (Eq. \quad 01)$$

where K_{max} is the kinetic energy carried by a photoelectron flying toward the anode, h is the Planck's constant, f is frequency, and W is the work function. The Planck's constant is therefore the slope of Eq. 01. Is this equation universally true? Fig. 01 gives a negative answer.

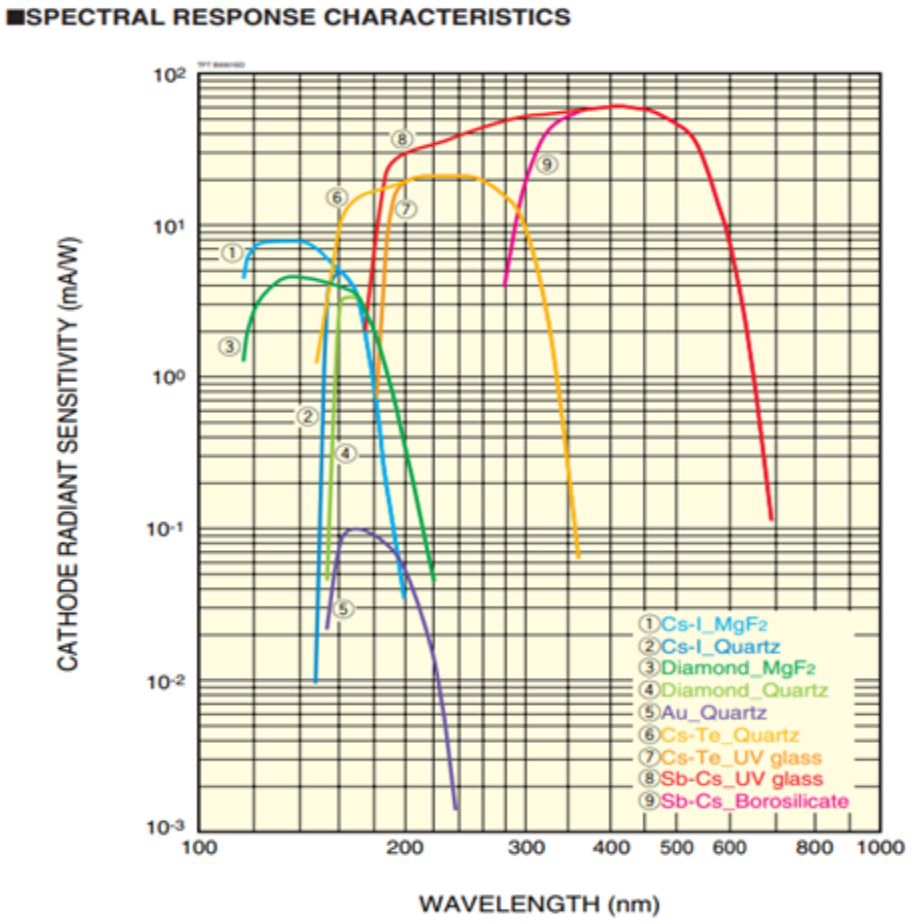

Source credit
https://www.hamamatsu.com/resources/pdf/etd/Phototubes_TPT1001E.pdf

Fig. 01

Every curve in Fig. 01 show drooping more and more toward higher and higher frequency, i.e., shorter and short wavelength of the incident light. Even more severely, at the very high frequency end, the supposed kinetic energy of the flying electrons, interpreted from the value of current, gets more and more reduced. Take curve 6 for example. Its linearity can be said best kept only between 360 nm (8.33×10^{14} Hz) and 330 nm (9.09×10^{14} Hz). Beyond 330 nm, the slope begins prominently deviated from the previous slop. At 260 nm (11.54×10^{14} Hz), the curve begins going flat. At 180 nm (11.54×10^{14} Hz), the curve goes downhill, meaning current, or equivalently the supposed K_{max}, rapidly diminishes; the concept of Planck's constant is made completely disappear. Indeed, even in the segment between 360 nm and 330 nm, the curve's slope shows no constant value but varying, although barely noticeable. When all these curves show so dominantly deviated from what Eq. 01 preaches, how can we accept this equation as having been written by a correct theory?

The theory guiding the establishment of Eq. 01 is not only challenged by experimental data, but it also provokes challenges against itself. let us examine the following few more arguments.

Argument Two *The theory of relativity fails to support the concept of quantum.* Overwhelmingly, photon has been advocated in modern physics to exist as quantum, which means a certain kind of material that is in the form of pure energy and with zero rest mass. That material can have zero rest mass is promoted and warranted by Einstein's relativity. If relativity can be shown as being self-refuted, the concept of zero rest mass for material will lose its base to stand. Subsequently, the concept of quantum loses its strongest protective umbrella. So unfortunately to this concept, indeed, relativity is self-refuted [1].

Argument Three *The concept of photon itself is self-refuted.* If photons are said to be packets comprising the moving train of light, then, by what a packet means, photons must be separated between each other within the train, both timewise and space-wise. So separated, if true, but due to the light's nature of being a wave, there must be at least one extra wave propagating along with this train of light, or train of packets. This extra wave must have frequency that is different from what each light packet carries. It is such extra wave that plays the role to suppress the train of light every so often space-wise and timewise. In other words, the existence of packets in a light train can only stir up wave interference. Interference of waves must produce beat. Has the science world ever claimed that beat is inevitable in any beam of pure light? Someone may object to this analysis with an argument that if the packets can randomly distribute themselves in the train of light, obvious beat cannot be found in our observation. However, a laser beam is a beam of pure light with well controlled coherence over phase when emitted. Who has detected any beat in laser light? Therefore, with the absence of beat in a light train, no separation within a finite light beam can be declared, and subsequently the possibility for packet to be distinguished between one and another is removed.

Argument Four T*he explanations proposed by modern physics between photoelectric effect and Compton effect fail each other*. According to the popular explanation based on quantum, upon absorbing the energy and momentum from a photon from the anode direction, an electron is excited to fly away from the cathode toward the anode (Fig. 02). This explanation literarily gives

people an idea that a recipient of certain momentum must move in a direction opposite to what the momentum exerts. Why must momentum carried by photon violate Newton's mechanical principle? Either it is the photon itself directly violates the principle, or the electron becomes weird because of the influence of the photon. Maybe someone argues that it is how the electron is destined to do because of the bias voltage between the two electrodes. The problem is that, as witnessed by segment b of the curve in Fig. 03, the flying also happens even when the bias voltage in many cases is zero or even negative. Besides violating the Newton's mechanical principle, the theory behind Eq. 01 also presents a challenge to the explanation on Compton effect, which also needs the concept of quantum to pave the way for people's acceptance.

In explaining the secondary wavelength found in the scattered X-rays (Fig. 04), Compton first listed the following two equations according to the principle of conservation of momentum from Newton's mechanism theory:

$$p_0 = p_1 \cos\theta + p\cos\emptyset \qquad (Eq.\ 02)$$

$$p_1 \sin\theta = p\sin\emptyset \qquad (Eq.\ 03)$$

where Eq. 02 contains all the momentum components projected on the X- axis and Eq. 03 contains all the momentum components projected on the Y-axis and further, all p's are symbols for momentum.

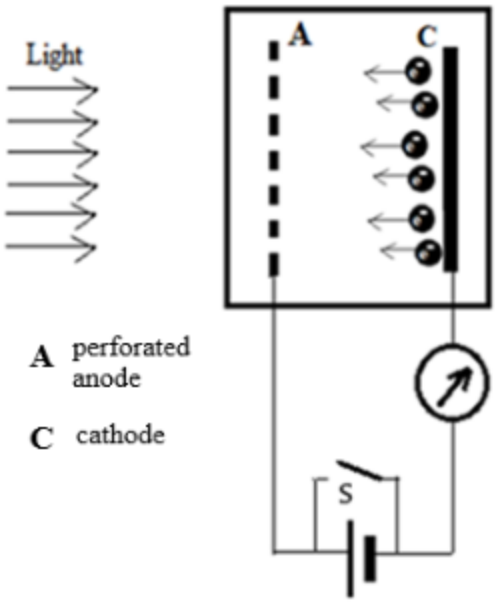

Fig 02 Simplified diagram for photoelectric effect

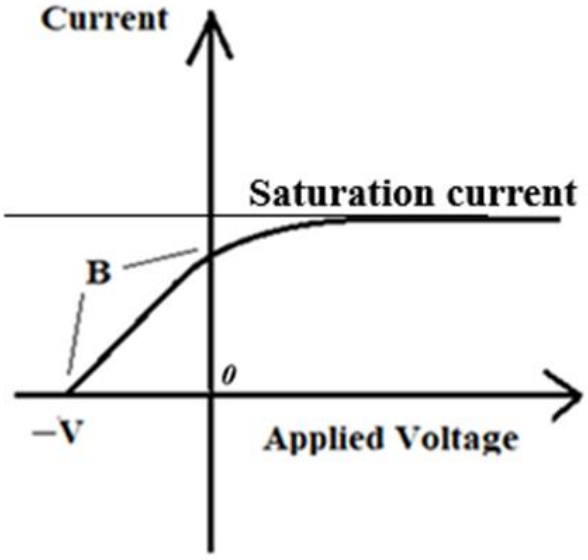

Reversed voltage is needed to stop the current shown in section B

Fig 03 Current *vs* applied voltage in photoelectric effect

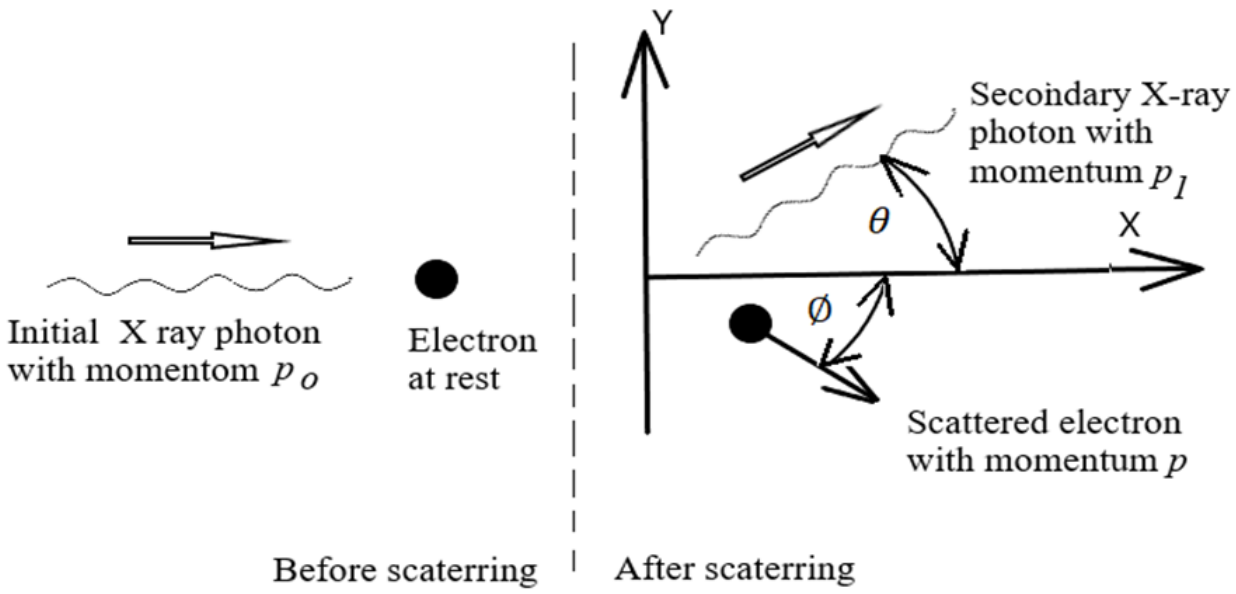

Fig. 04

Disregarding Compton's application of relativity in his further work (omitted here) on this topic, at least he felt only Newton's mechanics principle could warrant him to have these two equations correctly established. Obviously, in so pursuing, neither the secondary X-ray photon nor the scattered electron was assumed by him to move in the direction against the movement of the incident X ray photon.

The explanations from the photoelectric effect and Compton's scattering effect share one thing in common: an electron is excited by an incoming photon and resulted in a change of its location as well as moving state. However, both explanations thus have forced us to select one, and one only, from the following choices as a correct conclusion:

(1) Both explanations are mistaken,
(2) One of them is mistaken and the other one is correct,
(3) They both are correct.

It is obvious that choice (3), a choice for a contradicting pair, cannot be a correct conclusion, although it is a choice firmly held by the modern physics. Then, how correct the choice (1) or (2) would be? It is the purpose of this article to find out.

Argument Five About a *Finite Linear Dimension for a Quantum.* If a light beam has finite length, the total energy contained by this beam must be finite. Then, if the energy carried by each quantum is also finite, quantum theory must accept that the number of quanta, or photons, in this beam must be finite, regardless of how huge this number can be. All these must lead to

conclude that each quantum must have finite spatial dimension. So far, this author is unable to find article from any authoritative science institution showing firm information regarding the finite dimension of a quantum. When a reader tries to pursue this information, the answer usually is vague, such as" do not take it too literarily". On the other hand, however, if the contemporary popular explanation on the photelectric effect based on quantum is correct, such information is indisputably revealed in such explanation. We will find it out at the end of this article. Sadly, though, the finding can only come back to jeopardize the quantum theory's claim.

2. What Is There Helping the Electron's Defiance?

When the atomic structure is explored, the contemporary science dominantly believes that all electrons in an atom have high-speed circular orbital movement surrounding a nucleus. Relying on the centrifugal force produced by the orbital movement is how these electrons can successfully resist the attractive Coulomb force from the nucleus. Now, a question cannot help but presents itself to us: How reliable is such force in helping each electron sustain its orbital movement about the nucleus? It is also said that each electron has many different sizes of orbit. Jumping from one orbit to another, the electron releases (or absorbs) energy, which becomes light that gives us information about its orbit jumping. How compatible is such a view of light creation to our comprehension on how EM (electromagnetic) waves are created? We all know that light is EM waves with wavelengths in the visible range.

For an electron that jumps back and forth one time between the same two locations in one second, we say it would produce an EM pulse of 1 Hz. If it repeats the same manner of jumping multiple times in a longer time, we say it creates an EM wave of 1 Hz. The same logic would lead us to some statement like this: for an electron that jumps back and forth 1×10^{15} time in one second between the same two locations, we say it would produce an EM wave of 1×10^{15} Hz. Then, here comes the trouble if it is said that a light being produced due to the orbit jumping has a frequency of 1×10^{15} Hz. Concerning such light, which of the following statement is true?

(1) The electron completes the orbit jumping only one time, but instead of producing a pulse of 1 Hz, it produces a wave with a rate of certain kind of variations, such as 1×10^{15} (crest +trough), per second.

(2) The electron completes the back and forth jumping between the same two orbits at a rate of 1×10^{15} time/second. The light is produced on its way between the two orbits, but the orbital movement itself produces no light.

Statement (1) is obviously unacceptable because in the one-time pulse we find no source that could have driven the happening of certain kind of variation to be repeated 1×10^{15} times per second. Statement (2) obviously fails to include the time needed for the completion of the orbital movement in the frequency calculation. It is unacceptable either. As a matter of fact, the concept

of light produced due to or between orbital jumping is not found having been proven by experimental fact even though such claim has been circulating for a century.

So, if the above two statements cannot stand well, but the orbital movement must be imagined as the only mechanism to maintain the electron's independent life in an atom, why not just allow the orbital movement itself to possess the capability of light producing? In this way, light is given birth in a way more compatible to what we understand how EM wave is agitated to appear. So, after completing one orbit about the nucleus, the electron completes one period of movement and comes back to the same orbital starting point. As it moves, it must cause change of electric field in its vicinity. Subsequently another electron a distance away from this circulating one, if close enough, must sense an electric field variance coming at its way. The frequency it senses about the pace of this variation must match the periodical displacement made by the circulating electron. Of course, it is commonly known that nature must couple the change of an electric field with a change of magnetic field. So, with an angular speed of 1×10^{15} (2π)/second about the nucleus, this circulating electron lets the other electron at a distance away sense an EM radiation of frequency of 1×10^{15} Hz. Because the variation is caused by a circular movement, the variation sensed by the other electron is therefore a wave that can be described by a sinusoidal equation. Next, let us further using some data related to a sodium atom to continue our exploration.

The characteristic wavelength *l* of sodium-vapor lamp is 589 nm. The frequency matching this wavelength is 5.09×10^{14}Hz. The radius of a sodium atom is $0.227\ nm$. If an electron in a sodium atom is to generate a light wave of frequency of 5.09×10^{14}Hz, it must complete 5.09×10^{14} cycles of orbital movement in one second. Assuming the electron having been revolving about the nucleus on the biggest orbit in the atom, the linear speed v_e of the electron so moving is

$$v_e = 2\pi \times 0.227 \times 5.09 \times 10^{14}\text{nm/sec} = 726\text{km/ sec} \qquad (Eq.\quad 04a)$$

The centrifugal force F_c experienced by this electron should be

$$F_c = m_e \cdot \frac{\left(726\text{km}/_{sec}\right)^2}{0.227nm}$$

$$= 2.11 \times 10^{-29}\,N \qquad (Eq.\quad 04b)$$

where $m_e = 9.11 \times 10^{-31}kg$ is the mass of the electron. Of course, the force maintaining the electron's orbital movement comes from the Coulomb force F_e between the electron and the nucleus. Since the number of electrons and the number of protons are always equal in a neutral atom regardless of the atomic number, averaged out, we can assume the Coulomb force acting on the electron in our attention is from one proton. So, we have

$$F_e = -k\frac{q \times q}{r^2}$$

$$= -\left(9.0 \times 10^9 N \cdot \frac{m^2}{C^2}\right) \cdot \frac{(1.6 \times 10^{-19} C) \times (1.6 \times 10^{-19} C)}{0.227 nm^2}$$
$$= -1.014 \times 10^{-7} N \qquad (Eq.\ 05)$$

where $k = 9.0 \times 10^9 N \cdot \frac{m^2}{C^2}$ is the Coulomb constant, and $q = 1.6 \times 10^{-19} C$ is the charge per electron.

Eq. 05 shows that the force F_e is way bigger than F_c shown in Eq. 04b. This figures plainly tell us that no centrifugal force produced by orbital movement can be strong enough to enable the electron to defy the Coulomb force from a proton in the nucleus. Something else must be there helping. Then, what is that something?

In reasoning what causes gravity as well as how the frequency shift equation can be concluded from the Ives-Stilwell experiment, a hypothetical substance called Aether no doubt satisfactorily helps us solve the mysteries [2][3]. The solutions on these mysteries should therefore conversely provide us with a strong inference claiming the existence of Aether. The inference is made on the reliance of the omnipresent permeation of Aether in both the microworld and macroworld.

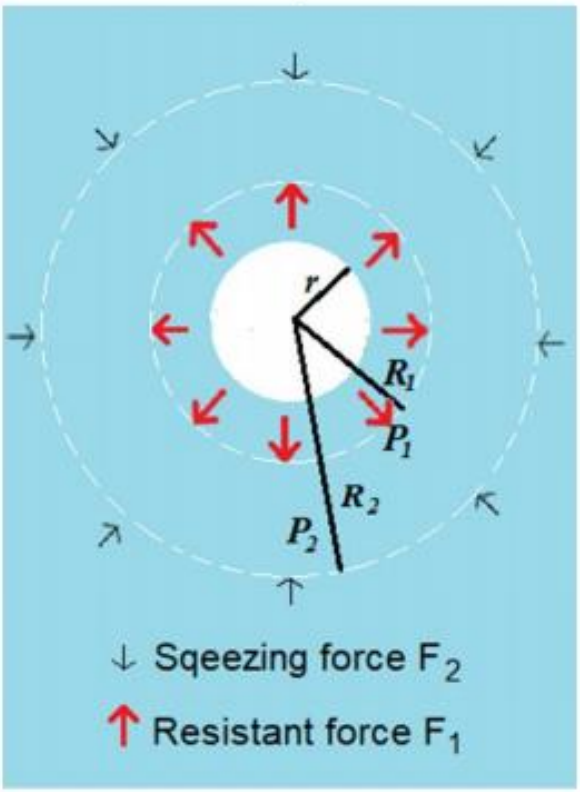

Fig. 05 Compressing force and resisting force acting over a bubble inside a fluid body

In exploring how Aether as a fluid manifests its presence via gravitational phenomenon, we reason that with respect to any two concentric spherical surfaces of radius R_1 and R_2, of which the center is identical to the center of a solid sphere, the pressure (force per unit area, either pushing in or pushing out) over their surfaces maintains the following relationship:

$$P_1\,(4\pi R_1^2) = F_1 = F_2 = P_2\,(4\pi R_2^2) \qquad (Eq.\ 06)$$

where P_1 is the pressure found on the surface of the R_1 sphere, and P_2 is the pressure found on that of R_2 (Fig. 05), the F_1 and F_2 represent the total force over the complete surface of each corresponding sphere.

From Eq. 06, we further have

$$\frac{P_1}{P_2} = \frac{R_2^2}{R_1^2} \qquad (Eq.\ 07)$$

Then, we can further apply this relationship to write

$$F_1 = F_2 = \cdots = F_n = P_{n=} 4\pi R_n^2 \qquad (Eq.\ 08)$$

where P_n is the pressure on the surface of the sphere of radius R_n. As $n \to \infty$, P_n on the surface of R_n is called the intrinsic pressure of Aether, which is a constant. In exploring the reason of gravity, this intrinsic pressure is found to be $P_0 = 1.0 \times 10^{12}\ {}^{kg}/_{cm^2}$. In the world with a linear scale of 1×10^{-8} m or larger, the Aether pressure is considered displaying its intrinsic pressure. With the intrinsic pressure so shown, we can easily find through calculation how the Aether's pressure can rapidly escalate itself in the world of atoms or in the vicinity of a nucleus.

When chemical elements are in their liquid or solid state, the shortest distance between atoms is usually in the order of $\times\ 10^{-10}$ m. In gas state, the average shortest distance between atoms is in the order of $\times\ 10^{-9}$ m. Since we are studying the sodium vapor light, we can regard the distance between the nucleus and the most remote electron in the atom to be in the order of $1 \times 10^{-9} m$. At such a distance, the Coulomb force F_{cl-1} between this electron and one of the protons from the nucleus can be found as

$$\begin{aligned} F_{cl-1} &= -k\frac{q \times q}{r^2} \\ &= -\left(9.0 \times 10^9 N \cdot \frac{m^2}{C^2}\right) \cdot \frac{(1.6 \times 10^{-19} C) \times (1.6 \times 10^{-19} C)}{(1 \times 10^{-9} m)^2} \\ &= -0.23 \times 10^{-7} N \qquad (Eq.\ \ 09) \end{aligned}$$

At the same distance from the nucleus, the out-pushing pressure P_1 of the Aether fluid should be

$$\begin{aligned} P_1 &= \frac{P_0 \times (1 \times 10^{-8} m)^2}{(1 \times 10^{-9} m)^2} \\ &= 1.0 \times 10^{19}\ {}^{N}/_{m^2} \qquad (Eq.\ \ 10) \end{aligned}$$

The corresponding out-pushing force F_{out} of Aether exerted on this electron should be

$$F_{out} = \sigma P_{1\cdot} = \sigma \cdot 1.0 \times 10^{19}\ {}^{N}/_{m^2} \qquad (Eq.\ \ 11)$$

where σ is the area of the large circle of an electronic sphere (an assumed shape), and this large circle is perpendicular to the radius from the nucleus. However, the out-pushing force is not the floating force for the electron, because, immersed in the fluid, the electron also receives an in-pushing force from the Aether pressure from the other side, in the direction toward the nucleus. The net force difference between the out-pushing force and in-pushing force is the floating force this electron experiences. Detailed calculation of the floating force can be found in Appendix II

at the end of this article. The outcome of Eq. 11 is just to give us an initial idea what can be a potential candidate in the scene helping the electron resist the sinking caused by the Coulomb force from a nucleus. Centrifugal force is too weak to be the candidate.

3. The Ward Where Light Is Generated

Since a sodium atom has 11 electrons, we cannot simply take what Eq. 05 portrays as the entire scene of the distribution of the Coulomb force interaction between all electrical charge particles in this atom.

In appendix I, there shows an analysis concerning the one electron that is the most remote one from the nucleus for each atom at the surface of a material chunk of sodium. Under the joined action from the Coulomb force from 11 protons and the Aether's out-pushing pressure contributed by 23 nucleons, this electron has the weakest force bonding it to the atom. If the most remote electron happens to belong to the atoms that form the outmost surface of a material body of sodium, this electron should have high chance to drift away from the grip from its atom. But, of course, eventually at a distance far bigger than the normal radius of a sodium, the coulomb force still catches up and stops it from a spontaneous permanent escape. However, at that specific distance, this electron no longer belongs to the atom which once "claims" owning it. But instead, it belongs to every atom at the outmost surface of the material body. Each of the atoms at the surface has the same fate as the one we just mentioned: their most remote electron drifts away. All these drifting-away electrons form a cloud hovering over the entire material body. The height of their hovering depends on the balance between the Aether's out-pushing force and the Coulomb force summed up from all the protons and electrons of the entire material body.

Besides the atoms that has formed the outmost surface of the material body, no other atoms would have its electron drifting away. It is because the atoms at the outmost surface, also closely packed together with a radius of 0.227 nm between each other, already organize an envelope of higher pressure of Aether that can present a blockade pushing back any out-drifting electron from inside.

With one electron egressing to the cloud, each of the surface atom together would sure convert the cathode sheet in the photoelectric experiment into a disk of uniform charge θ per unit area . Comparing to the size of an electron, such a disk can be considered infinite. The electric field E over a surface of an infinite charged sheet is given as

$$E = {\theta}/{2\epsilon_0} \qquad (Eq. \quad 12)$$

where ϵ_0 is the permittivity of the free space. Therefore, within quite a big distance from the surface of the cathode sheet, before any bias voltage appears, each electron in the cloud should always experience the same electrical attractive force F_{e1} from the cathode, which is

$$F_{e1} = Eq = \frac{\theta q}{2\epsilon_0} \qquad (Eq. \quad 21a)$$

For a cathode sheet made of sodium, we have $\theta = +2.11 \times 10^{13} C/m^2$ (See Appendix III). Therefore, to this electron, according to Eq. 21a, we have

$$F_{e1} = \frac{\theta q}{2\epsilon_0}$$

$$= \frac{2.11 \times \frac{10^{13} C}{m^2} \cdot 1.6 \times 10^{-19} C}{2 \times 8.85 \times \frac{10^{-12} C^2}{N.m^2}}$$

$$= 1.9 \times 10^5 N \qquad (Eq. \quad 21b)$$

If we set the floating force F_{fl} received by the electron as concluded in $Eq - II - 11$ (from Appendix II) equal to F_{e1}, we have

$$\frac{40\pi R}{1.0 \times 10^{-8}\, m - H} \cdot N = 1.9 \times 10^5 N \qquad (Eq. \quad 21c)$$

where R is the radius of the electron with an assumed shape of a sphere. Eq. 21c solved with respect to H, we have

$$H = (1.0 \times 10^{-8} - 6.61 \times 10^{-4} R)m \qquad (Eq. \quad 21d)$$

Since $1.0 \times 10^{-8}\, m$ is the distance from the nucleus to where the intrinsic pressure dominates (Fig-II-01), and H is from the electron to where the intrinsic pressure dominates, so, the distance l_{e-n} between the electron and the nucleus in the outmost surface of the cathode should be

$$l_{e-n} = 1.0 \times 10^{-8} m - H = 6.61 \times 10^{-4} R \cdot m = 6.61 \times 10^5 R \cdot nm \qquad (Eq. \quad 21e)$$

It is at about this distance l_{e-n} from the cathode that an electron receives a balance treatment from two forces acting from opposite direction. In many ways, this range is like a free space to the electron. If it is to move back and forth because of whatever reason at speed 726km/sec (Eq. 04a) and at a frequency of $1.0 \times 10^{15}\text{Hz}$, it can have enough room for the freedom. In doing so, each of its one-way trip is

$$\frac{726\text{km/sec}}{2 \times (1.0 \times 10^{15}\text{Hz})} = 3.63 \times 10^{-10}\text{m} = 0.367\text{nm} > 0.227\text{nm} \qquad (Eq. \quad 22)$$

The figure 0.227nm above is the radius of the sodium atom. In a moving state matching all these data, the electron is producing a blue light, but to produce such light, an electron must first have enough room to oscillate. Now, the room is provided in space away from the entire material chunk. Of course, conversely, an incident blue light will entice the electron to be in a moving state that matches all these data.

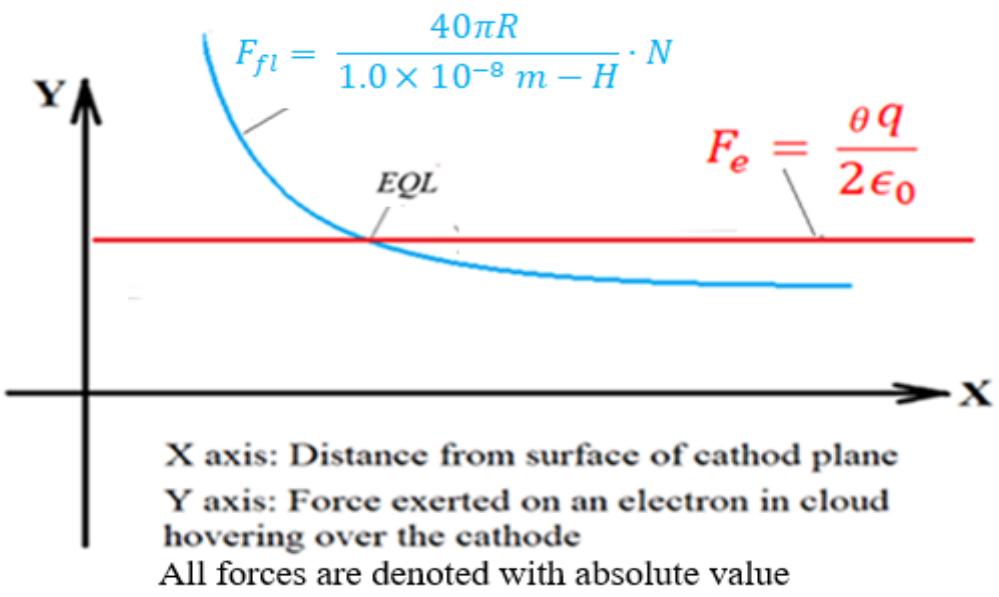

Fig. 06

In deriving the floating force F_{fl} shown by $Eq - II - 11$, we only use one nucleon for the center as a reference for all concentric spheres. However, in real life, the floating force that an electron experiences over the cathode surface is a sum of contribution from all nucleons in the entire material body of the cathode although each from different distance. Given all these considerations, l_{e-n} in Eq. 21e should have a bigger value. In other words, the point where the electron experiences balance between forces should be larger than what Eq. 21e shows.

While the electrical force near the surface of an infinite plate keeps constant, the out-pushing pressure of the Aether fluid retains the character of being inversely proportional to distance. Such different behaviors from these two forces lead us to an idea that, at a certain distance from the cathode surface, there should exist a point we call equilibrium point, abbreviated as EQL, between there two kinds of force. At this point the floating force and the Coulomb force acting on an electron are equal to each in magnitude and opposite in direction (Fig. 06). It is this idea that enables us to assert the establishment of Eq. 21c.

The curves drawn based on the behave shown by Eq. 21a and Eq.II-11 tell us that within the space between the EQL and the cathode surface, the Aether's floating force is stronger than the electrical force, while in space beyond the EQL and away from the cathode surface, the electrical force is stronger than the floating force.

Let us imagine an electron located at a neutral spot P in a space that is free of any foreign interference, and this electron is shone by a light ray (Fig. 07). At the completion of the first half cycle "a" from a light wave, this electron is forced by the electromagnetic force to relocate to spot Q

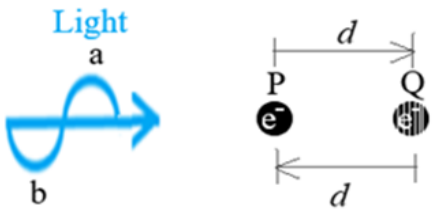

Fig. 07

through a distance d. According to the common knowledge in physics about wave, at the completion of the second half cycle "b", the electron must return to spot P from Q. Frequency of the light waves has no effect on such outcome. However, if the environment of the space is not free, but the electron must overcome certain resistance in its back and forth movement, the situation is different. At the end of the returning trip, the electron should fail to return to spot P. Indeed, it may not even have reached Q due to the energy loss in its forward trip. This pattern of movement should be true to the electrons in the photoelectric effect experiment when excited by light.

With all preceding preparation, we now can explain several characteristic phenomena associated with the photoelectric effect. These phenomena include the following three:

(A) The photoelectric current *I* is in proportion to the frequency of the incident light *f*, or simply $I \propto f$

(B) There exists a threshold frequency f_0 below which no photoelectric current can be produced.

(C) Once the photoelectric current reaching a saturation value, it would fundamentally stop increasing regardless of the increase of the bias voltage V across the electrodes. However, the current does increase with the intensity of the incident light as V is held constant.

4. Regarding $I \propto f$

Suppose for some reason (explore a little later) in one complete cycle of the light wave, an electron's outbound (away from the cathode) trip gains an extra distance *d* more than the inbound trip. Then, if incident light beam A shines on an electron with frequency f_A will enable the electron to gain a total net distance $D_A = df_A$ in one second. By the same token, another light beam B of the same intensity but frequency f_B would enable this electron to gain a total net distance $D_B = df_B$ in one second. Because the light intensities of both A and B are the same, both should also be able to motivate equal numbers of electrons *n* in every period of each of these two beams to cross the same area that is perpendicular to the line between the two electrodes. Since the strength *I* of an electrical current is determined by the number of electrons moving across a unit area per unit time, we would have

$$I_A = \left(\frac{nq}{second}\right) df_A \qquad and \qquad I_B = \left(\frac{nq}{second}\right) df_B \qquad (Eq.\ 23)$$

Consequently, we have

$$\frac{I_A}{I_B} = \frac{f_A}{f_B} \ , \quad or \quad I \propto f \qquad (Eq.\ 24)$$

Of course, as what has been commented regarding Fig. 01, the relationship shown by Eq. 24 can only cover a limited range of frequency.

5. Why Is There a Threshold Frequency f_0 ?

When the first half cycle *a* of the light wave happens to have driven an electron at the EQL to move toward the cathode, this electron would simultaneously do four things: (1) absorbing the incoming energy E_a in a sinusoidally progressive manner, (2) storing mechanical potential energy $E_{P,a}$ through building up of floating force in the Aether fluid, (3) releasing electrical potential energy $E_{e,a}$ with respect to the charge cathodes sheet that is considered infinite, (4) spending energy $E_{r,a}$ to overcome dragging force of the Aether fluid. $E_{r,a}$ cannot be stored in any manner. Once gone, it is gone, no matter what.

In the next half cycle *b*, the electron is driven to move away from the cathode. During this process, the follow four things happen to this electron: (1) absorbing the incoming energy E_b, (2) releasing mechanical potential energy $E_{P,b}$ through the recoiling action enabled by the Aether's floating force, (3) building up electrical potential energy $E_{e,b}$ with respect to the infinite charge sheet, (4) spending energy $E_{r,b}$ to overcome fluid resistance. $E_{r,b}$ cannot be stored in any manner. Once gone, it is gone, no matter what.

So, regarding the half cycle *a*, we can set up the following equation

$$E_a = \int_{s_1}^{s_2} B(\frac{M}{s})ds + \int_{s_1}^{s_2} -\frac{\theta q}{2\epsilon_0}ds + E_{r,a} \qquad (Eq. \quad 25)$$

where $\frac{M}{s}$ in the first integral is the floating force of the Aether in the vicinity of a nucleus. This force is written according to Eq-II-11 (from Appendix II), with $M = 40\pi R$, $s = 1.0 \times 10^{-8}\ m - H$, and H is the distance between the electron and where the Aether's intrinsic pressure begins to dominate. As to B, it is a coefficient of constant value. B is needed because the floating force at *any point* in the space over the cathode is not caused by a single nucleus but a collection of nuclei that have been lined up in the cathode. Each nucleus has different distance from this point. Therefore, the floating force at this point is actually a composite force of numerous component force, each of which is contributed by a nucleus according to its own location. This force so resulted through superimposition has equipotential characteristics (Fig.08): It has the same value at any point along a line that is parallel to the cathode surface. But such value is different from line to line. Further, s_1 in the integral is where the electron starts moving, s_2 is where the electron is when the first half cycle, named as *a*, ends. Both are measured from the cathode surface.

With respect to the half cycle *b*, we can set up the following equation

$$E_b = \int_{s_2}^{s_3} -B(\frac{M}{s})ds + \int_{s_2}^{s_3} \frac{\theta q}{2\epsilon_0}ds + E_{r,b} \qquad (Eq. \quad 26)$$

where s_3 is the point that the electron will reach at the end of the half cycle *b*.

Since $|E_a| = |E_b|$, Eq. 25 and Eq. 26 together give us

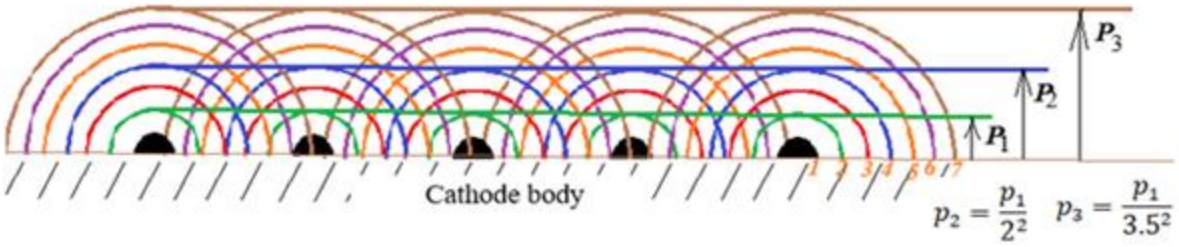

Above is a schematic suggestion on the proportional relationship caused by distance difference between potential value P's. What is suggested here is some simplified presentation.

The actual value at each chosen point should be more complicated than suggested here because of the superpostion of influence from all sources. However, because the superposition of all these quantities are straightforwardly linear, the relationship mathematically suggested above should be kept for all horizontal lines so long as the cathode surface can be regarded as infinite .

Fig. 08

$$\left|\int_{s_1}^{s_2} B(\frac{M}{s})ds + \int_{s_1}^{s_2} -\frac{\theta q}{2\epsilon_0}ds \ + \ E_{r,a}\ \right| = \left|\int_{s_2}^{s_3} -B(\frac{M}{s})ds + \int_{s_2}^{s_3} \frac{\theta q}{2\epsilon_0}ds \ + \ E_{r,b}\ \right| \quad (Eq.27)$$

Since both $E_{r,a}$ and $E_{r,b}$ must carry the same sign on each side of the equation, we can have

$$\left|\int_{s_1}^{s_2} B(\frac{M}{s})ds + \int_{s_1}^{s_2} -\frac{\theta q}{2\epsilon_0}ds\ \right| + (\ E_{r,a}\ -\ E_{r,b}) = \left|\int_{s_2}^{s_3} -B(\frac{M}{s})ds + \int_{s_2}^{s_3} \frac{\theta q}{2\epsilon_0}ds\right| \quad (Eq.28)$$

If $E_{r,b} = E_{r,a}$, we will have

$$\left|\int_{s_1}^{s_2} B(\frac{M}{s})ds + \int_{s_1}^{s_2} -\frac{\theta q}{2\epsilon_0}ds\ \right| = \left|\int_{s_2}^{s_3} -B(\frac{M}{s})ds + \int_{s_2}^{s_3} \frac{\theta q}{2\epsilon_0}ds\ \right| \quad (Eq.29)$$

Then further, that the following two distances are equal is concluded from Eq. 29:

$$|s_3 - s_2| = |s_2 - s_1| \qquad (Eq. \quad 30a)$$

If s_1 is the point of EQL, Eq. 30a means s_3 is also the EQL. However, will this happen?

When the electron moves toward the cathode, it must encounter an ever-increasing pressure of the Aether, but moving away from the cathode in the second half cycle, *b*, its environmental pressure is ever decreasing. Therefore, the energy it needs to spend to overcome the drag is different in the two opposite trips and results in $E_{r,a} > E_{r,b}$. Subsequently, Eq. 28 will lead us to have

$$|s_3 - s_2| > |s_2 - s_1| \qquad (Eq. \quad 30b)$$

If $s_1$is the EQL point, Eq. 30b means s_3 is not the EQL, but a point beyond the EQL and further away from the cathode as shown in Fig. 09, a diagram with a closer look around the EQL

At s_3, the Coulomb force F_e is stronger than the Aether's floating force F_{fl}. when reaching s_3, the electron retains some potential energy ΔE due to $F_e - F_{fl} > 0$ with respect to the cathode surface. If the next cycle of EM wave arrives at the exact time the electron reaches s_3, the electron will move toward the cathode again but with an energy batch that is equal to ($E_a + \Delta E$). If this batch is big enough, the electron will be able to visit the previous spot s_2 again. If not, naturally, the electron will reach a location s'_2 that is a little more far away from the cathode's surface than s_2 (Fig. 09). Then upon the influence of the next half cycle which carries energy E_b, the electron will move away from the cathode again and also reach a new point s'_3 that is a little more far away from the EQL than s_3 due to the principle suggested by Eq. 30b. Mathematically we have

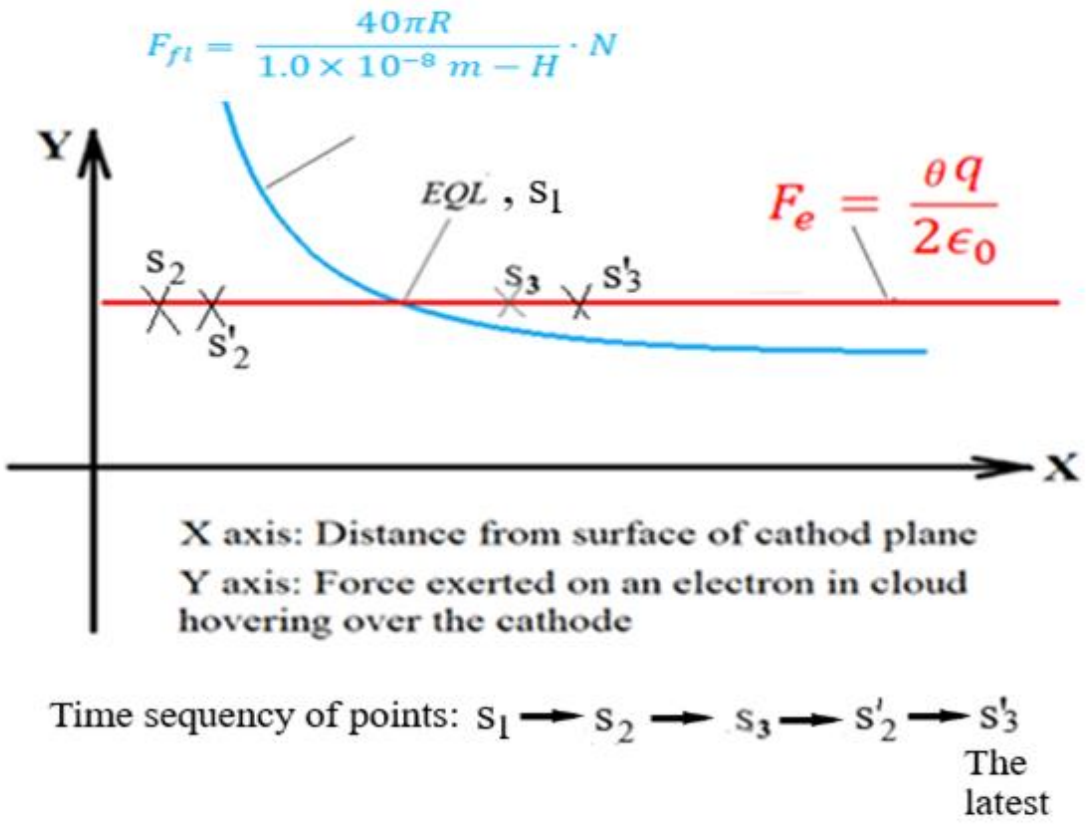

Fig. 09

$$|s'_3 - s_3| > 0 \qquad (Eq. \quad 31a)$$

or,

$$|s'_3| - |s_3| = d \qquad (Eq. \quad 31b)$$

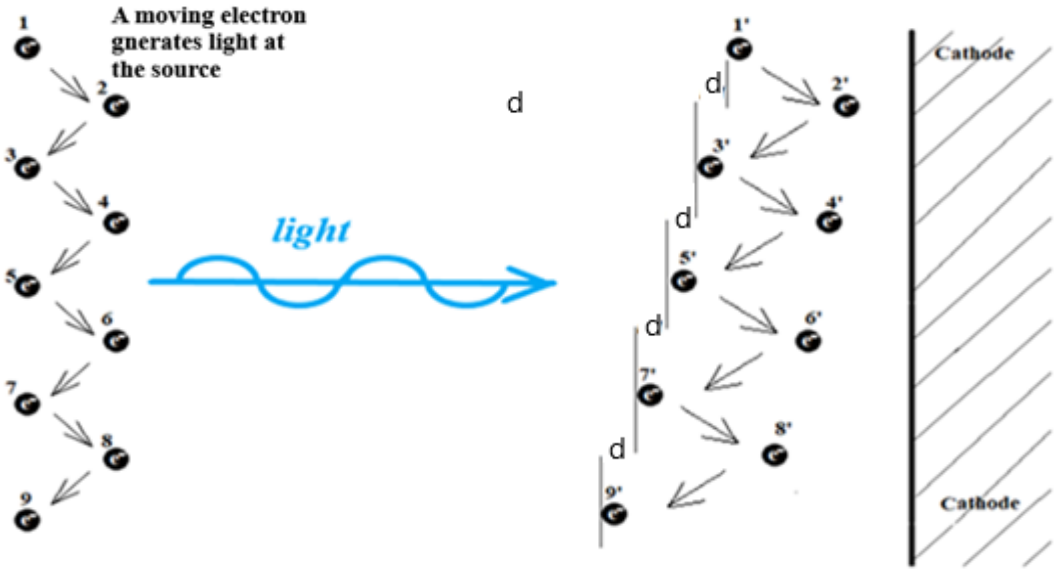

The above is a "break-down" of the moving trip of the same electron at the light source and at the cathode, respectively. What actually happens should be more properly represented by the picture below, where d = net gained distance.

Fig. 10 An electron at the cathode gradually gains distance as it corresponds to the movement of the electron at the light source

Eq. 31b means that the same electron gains an extra distance d at the end of the 2nd period of the light wave in comparison to what it went through at the completion of the first period. The incessant light excitation from a train of light wave then create an extra distance d at the completion of every period of the light wave. All these net distance gain of d will accumulate to an ever-increasing distance with respect to the cathode (Fig. 10). Eventually the electron is sent far away from the cathode until it reaches the anode and being disposed of there. This electron is called photoelectron.

Now, weather we can initially have $|s'_2| > |s_2|$ or $|s'_2| = |s_2|$, the key depends on the quantity of ΔE. Only if $\Delta \boldsymbol{E}$ **is *below a certain value***, then $(E_a + \Delta E)$ cannot be strong enough to send the electron back to s_2 but leave it at s'_2, and then can $|s'_2| > |s_2|$ be guaranteed. Since each trip of the electron's movement is closely governed by each of the half wavelength of the incident ME wave, that a statement *"*$\Delta \boldsymbol{E}$ ***is below a certain value***" means each of the half wavelength cannot be bigger than a certain value, which we herein designate as λ_0. Of course, "no bigger wavelength" is a direct interpretation of "no lower frequency". A threshold wavelength λ_0 therefore sets a **threshold frequency $\boldsymbol{f_0}$**, below which, no photoelectric current can appear.

The above answer for the riddle of a minimum frequency also suggests to us that the true nature of the so-called work function should have nothing to do with the atomic bonding energy. The energy lost seen accompanied with the production of photoelectron should be more appropriately understood as the energy loss caused by the Aether's fluid dragging resistance, i.e., the total sum of $E_{r,a}$ and $E_{r,b}$ from all cycles, i.e., $\sum(E_{r,a} + E_{r,b})$.

6. Saturation Current and The Bias Voltage

From all previous description, we can say that photoelectric effect is a spontaneous reaction so long as light is available and above a minimum frequency. What holds the key for the electron to get chance to get away from the cathode is the floating force of the Aether fluid. However, the photoelectron's journey is not completed by one single trip but multiple back-and-forth trips in a fluid that has an equipotential characteristic with its pressure, which is getting higher at distance closer to the cathode. When the photoelectrons are in the trip moving toward the cathode and must encounter higher force to push them back, they may highly likely move sideways. Any electron drifting sideways means a reduction of number of electrons inside the path covered by the light beam, and subsequently a reduction of the strength of the photoelectric current. To avoid such electron loss, of course, a foreign bias voltage is helpful. With such bias voltage, the sideway drifting is restricted because the electrons now can penetrate the equipotential barrier. The stronger is the bias voltage the better. However, the help of the voltage is only good up to a certain value. When the restriction has reached 100% efficiency, the sideway drifting of electron is zero, and high bias voltage is just a waste. When the bias voltage reaches its 100% efficiency, the current reaches its saturation value.

The bias voltage is unable to change the electron population in unit space in the cloud hovering over the cathode. The availability of such electrons is determined by the nature of the cathode material. On the other hand, the incident light does have another way to increase the photoelectric current. It is its intensity. A higher intensity of light can entice more electrons in the same cloud to move toward the anode and thus increase the current.

In short, the role of the bias voltage is only to help enforce the moving direction of the photoelectrons and has nothing to do to change the number of electrons in the cloud and thus has no influence on the value of saturation current.

7. Why Do Curves in Fig. 01 All Fail the Equation $K_{max} = hf - W$

All curves in Fig. 01 must show reduced current after the incident light goes beyond a certain frequency. The higher the frequency goes, the more severe the reduction appears. The relationship of $I \propto f$ is completely inapplicable there.

Electrons has mass, which must present inertia against any force that is to change the moving state it has been in. When an electron is summoned to join the photoelectric current by a light of frequency, say, $1 \times 10^{15} cycles/second$, it means this electron has to reverse its moving direction 2×10^{15} times every second in the entire of its journey flying toward the anode. One reversal of direction means one reversal of momentum carried by the electron. Gradually, as the frequency goes higher and higher, what is illustrated in the following paragraph becomes more and more pronounced, particularly at the end of the out-bound trip away from the cathode. Let us focus on such situation at the out-bound trip:

At the end of one of the half cycles, the energy impelling the electron is zero. However, at that instant, the electron's kinetic energy still has some nonzero residue, which must motivate the electron to move for some distance. The ever-decreasing pressure of the Aether in the out-bound trip even adds some favors to such sliding. However, before the electron can really come to a full stop, the second half cycle shines on, and by nature, it is to goad the electron to move in an opposite direction. To do so, now, this newly arriving cycle needs to spend some energy to curb the electron to a full stop before it can carry the electron to move in the way this half cycle intends. When the reversal of movement is mathematically feasible, however, this second half cycle would have already become weaker. The outcome is a slower movement and a shorter distance for the electron in the moving back trip. Slower movement and shorter distance of course result in reduced number of electrons crossing the same area in unit time for current calculation. Now, the electron's back and forth movement and the repetitive renewal of the half cycle of the light are out of synchronization. The higher the light increases its frequency, the more severe is the out of sync phenomenon, and each of the light's half cycle must spend more energy in overcoming the residue momentum left by the previous half cycle. This is what exactly all curves in Fig. 01 tell us. Clearly, the equation $K_{max} = hf - W$ cannot cover the out-of-synchronization problem in its explanation.

There is a mystery that the nowadays scientific world still pursues. It is the time lag between the incidence of radiation and the emission of a photoelectron. Someone claims being less than 10^{-9} second [4], while someone else claims being in 45×10^{-18} second [5]. With all that has been mentioned, we should say that the emission begins in no time but as soon as the arrival of the light. However, the success of an emission is another matter. A success of emission is signified by the registration of the start of the photoelectric current.

8. A Finite Spatial Dimension for Quantum Led by $E_{max} = hf - W$

The equation $E_{max} = hf - W$ is claimed to be established on an idea that quantum has no finite spatial dimension. However, beyond what it is aware of, this equation reveals its nature of asserting a finite spatial dimension for a quantum.

Any light beam must have a finite length and a finite amount of energy. This means that, if light is consisted of quanta, or packets of energy, and the energy content of each quantum is finite, the number of quanta embraced by this light beam must be finite. This is an ironclad logic in mathematics. As such, each quantum must be individually identifiable, countable, and measurable. However, preaching no finite dimension for quantum is one of the important topics of quantum theory. Now, let us investigate how Eq. 01 enables us to determine the finite linear dimension of a quantum.

Fig. 11 shows some physical drawing of a photo tube. If the base of the tube is 23 mm, the distance between the cathode and the anode can be estimated from the diagram as 8 mm. For the sake of convenience in calculation, let us take it as 10 mm. In an experiment with this tube, let the incident light has a frequency f of $1 \times 10^{15} Hz$, and the cathode material be sodium, of which the work function $\emptyset$ is 2.46 eV. According to conventional understanding, these data would lead us to get the energy K_{max} carried by a photoelectron flying toward the anode as

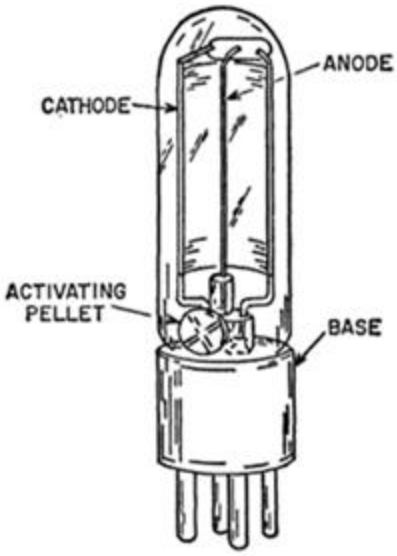

Typical construction of a vacuum phototube.

Credit source:
http://www.bitsavers.org/components/rca/1963_PT-60_RCA_Phototubes_and_Photocells.pdf

Fig. 11

$$K_{max} = hf - \emptyset = 1.68eV \qquad (Eq. \quad 32)$$

With this kinematic energy, the speed v of the flying photoelectron would be

$$v = \sqrt{\frac{2K_{max}}{m_e}}$$

$$= \sqrt{\frac{2 \times 1.68eV}{9.1 \times 10^{-31} kg}}$$

$$= 7.6 \times 10^5 \ {}^{m}/_{s} \qquad (Eq. \quad 33a)$$

The time Δt needed for the photoelectron to fly across the electrodes is

$$\Delta t = \frac{10x10^{-3m}}{7.6 \times 10^5\, {}^{m}/_{s}}$$

$$= 1.28 \times 10^{-8} seconds \qquad (Eq. \quad 33b)$$

With the same time interval Δt, the propagating light train would have filled a space with a length L that is calculate as

$$L = 1.28 \times 10^{-8} seconds \times 3 \times 10^8\ {}^{m}/_{s}$$

$$= 3.84m \qquad (Eq. \quad 34)$$

If the light shining on the cathode is never interrupted, and the space between the two electrodes is continuously filled with flying photoelectrons, $Eq.34$ would mean that the fulfilment of the space between the electrodes with photoelectrons needs the energy from a light train of the length of $3.84m$. This is so because the first electron now immediately next to the anode has consumed the energy of the first photon in the $3.84m$ light beam, and at the same instant the last electron in line now just starting leaving the cathode has consumed the energy of the last photon from the same beam. Since the wavelength λ of the beam of $1 \times 10^{15} Hz$ is 3×10^{-7}m, the total number of wavelength λ covered by this $3.84m$ light beam should be 1.28×10^7.

Since Eq. 01 warrants one quantum producing one photoelectron, we can imagine a scene so described in the following: A single file of straight line of photoelectrons is found between the two electrodes. This line of photoelectrons is made up by electrons lining up one after another. If there are *k* number of photoelectrons lining up between the two electrodes, there would be *k* number of quanta in the light beam of length of $3.84m$ for the consumption of these photoelectrons, and these *k* quanta also line up one after one in the beam correspondingly. Then, the length or the linear dimension L_q that each of the *k* quanta occupies would be

$$L_q = \frac{3.84m}{k} = \frac{1.28 \times 10^7 \lambda}{k} \qquad (Eq. \quad 35)$$

Fig. 12 shows some saturation currents in certain photoelectric experiment. For the light beam of $1 \times 10^{15} Hz$, the saturation current is $1.6 \times 10^{-6} Amp$. Before further investigation on this current, it should help to review the definition of current *I*. Since Eq. 01 is devised on the prospect that the photoelectric current is composed of electrons that all move in one smooth journey from the cathode to the anode other than multiple back-and-forth trips, the following definition of current well matches what Eq. 01 projects

$$I = nqvA \qquad (Eq. \quad 36a)$$

where n is the number of mobile charge carriers, or photoelectrons in our case, per unit volume, *A* is the cross-sectional area through which the photoelectrons pass, v is the speed at which the charge particles pass, and q is the electric charge each photoelectron carries. So, in comparison with Eq. 36a and since the distance between the two electrodes is 10 mm, the single line of photoelectrons between the two electrodes enables us to have

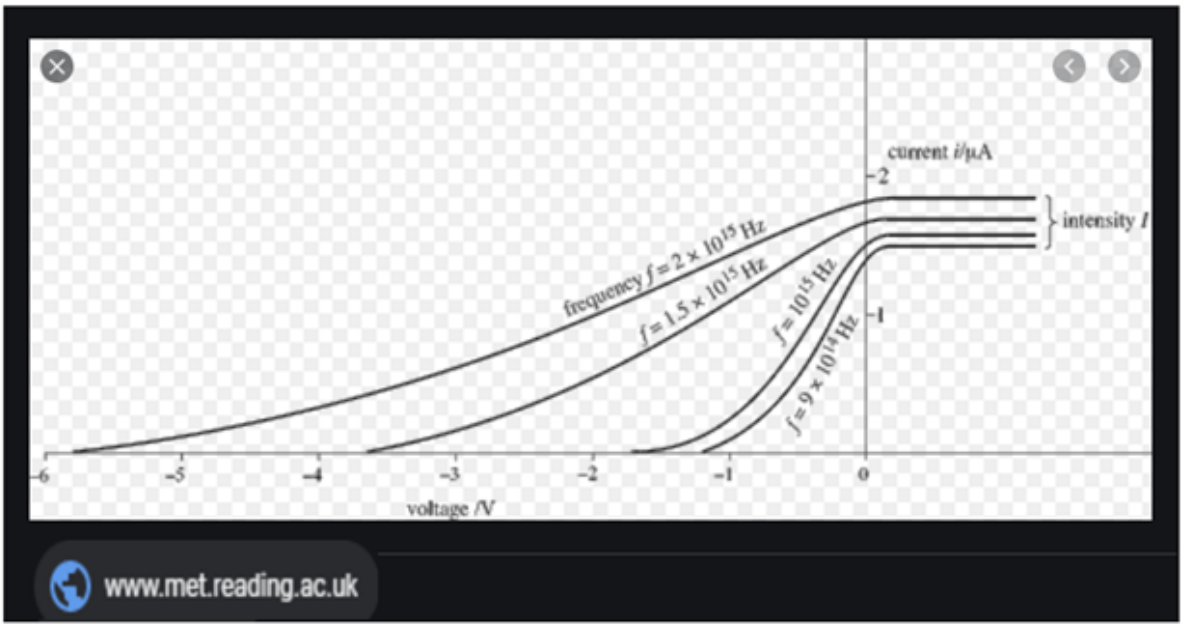

Fig. 12

$$nA = (\frac{k}{10 \times 10^{-3} m \cdot A})A = \frac{k \times 10^2}{m} \qquad (Eq. \quad 36b)$$

Subsequently, continued from Eq. 36a but with all numerical values in place, we have

$$1.6 \times 10^{-6} Amp = \frac{k \times 10^2}{m} \cdot (1.60 \times 10^{-19} C) \cdot (7.6 \times 10^5 \ {}^{m}/_{s}) \qquad (Eq. \quad 37)$$

Solving Eq. 37 with respect to k, we have

$$k = 1.32 \times 10^5 \qquad (Eq. \quad 38)$$

Replacing $k = 1.32 \times 10^5$ in Eq. 35, we have

$$L_q = \frac{3.84m}{k} = \frac{1.28 \times 10^7 \lambda}{1.32 \times 10^5} = \cong 97\lambda = 97(3 \times 10^{-7})\text{m} \qquad (Eq. \quad 39)$$

Eq. 39 means that every quantum in the light beam of 1×10^{15} Hz occupies a length of $97(3 \times 10^{-7})$m . This is a finite length that Eq. 01 entitles each quantum to have because of the speed of the electron that is given by this equation and as shown in $Eq. 33a$.

According to the quantum theory, a photon's energy E_{ph} in the light beam should be

$$E_{ph} = hf = 6.626 \times 10^{-34}\text{Js} \cdot \frac{f(cycles)}{sec} \qquad \text{(Eq. 40)}$$

Then, the energy contained by each cycle of light should be

$$\frac{E_{ph}}{f(cycles)} = 6.626 \times 10^{-34}\text{J} \qquad \text{(Eq. 41)}$$

With 97 cycles for one photon, the photon's energy E_q should be

$$E_q = \frac{E_{ph}}{f(cycles)} \cdot 97\ cycles = 6.626 \times 10^{-34}\text{J} \cdot 97 = 6.43 \times 10^{-32}\text{ J} \qquad \text{(Eq. 42)}$$

However, if we stop reasoning further at Eq. 40 but just directly replace $\frac{f(cycles)}{sec}$ with $1 \times 10^{15} Hz$ in this equation, we will have

$$E_{ph} = 6.626 \times 10^{-34}\text{Js} \times 1 \times 10^{15}\ Hz = 6.626 \times 10^{-19}\text{J} \qquad (Eq. \quad 43)$$

Both E_q from Eq. 42 and E_{ph} from Eq. 43 are supposed to mean the same thing: the energy of one photon, or equivalently, one quantum. But obviously, they now each shows some dramatically different value contradicting to each other. If quantum theory wants to convince people it is a trustworthy theory, it should oblige itself to clarify to people which of these two values, E_q or E_{ph}, can be genuinely endorsed by nature. Until then, we have to say:

One more self-refuted concept is found packed in the library of Modern physics.

Without Aether, nature must present us a huge impassible puzzle in explaining photoelectric effect. With Aether and the authority of classical physics, nature hands us a key to unlock this puzzle.

Now, if we go back to review the 3 questions below Fig. 04 on page 5 regarding argument four, we will find **answer (1) there should be the right choice**.

Appendix I

—Electrical Force Distribution in An Atom—

Fig. I-01 is drawn for the analysis of Coulomb force that is experienced by the most remote electron in a sodium atom. It is said that, with an atomic number of 11, a sodium atom has two layers of electron distribution plus one remotely located from the nucleus. The first layer, the one closest to the nucleus, has two electrons. The second layer, with larger distance from the nucleus, has 8. Then, the last one will stay quite remotely from the second layer. So, from the stand point of the most remote electron, the total pronounced Coulomb force from the nucleus exerting on it is from 9 protons, because the Coulomb force from 2 out of the 11 protons in the nucleus can be considered nullified by the 2 electrons in the first layer. Now, what genuinely exerting Coulomb force on this remote electron would be the attracting force from 9 protons and the repellent force from the eight electrons in the second layer.

The upper portion of Fig. I-01 is a 3-D illustration, and the lower portion is a 2D side view of the same scene. From this picture, we have the following data:

$$|AB|^2 = (mR)^2 + R^2 \qquad (Eq - I - 01)$$

where $m > 0$ is a coefficient that can be any value.

$$|AC|^2 = [(m+2)R]^2 + R^2 \qquad (Eq - I - 02)$$

$$\cos\alpha_1 = \frac{mR}{\sqrt{(mR)^2 + R^2}} \qquad (Eq. -I - 03)$$

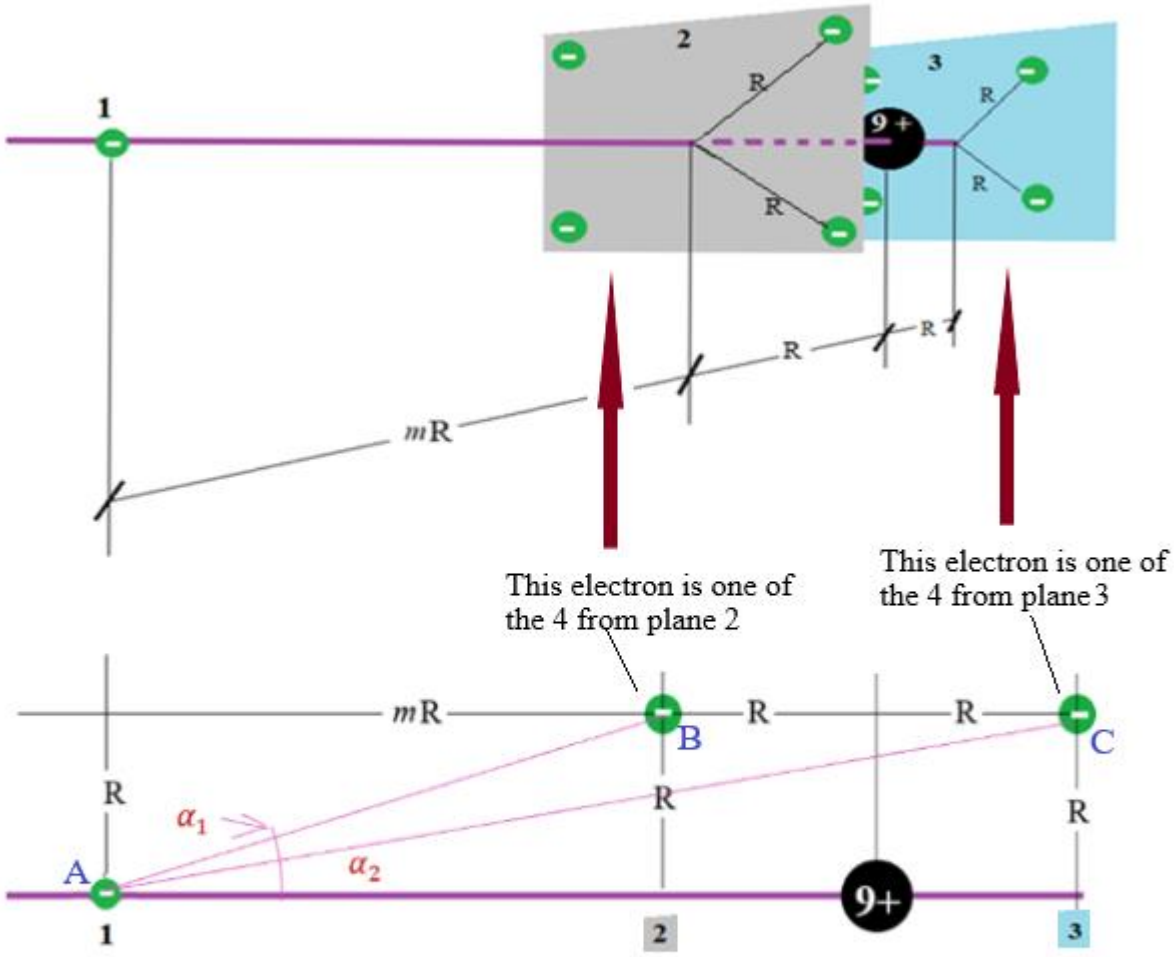

Fig. I-01

$$\cos\alpha_2 = \frac{(m+2)R}{\sqrt{[(m+2)R]^2 + R^2}} \qquad (EQ.-I-04)$$

Then, we set up the following equation for the total Coulomb force F_{tot} received by the most remote electron as

$$F_{tot} = Kq^2\{\frac{4}{(mR)^2 + R^2}\cdot\frac{mR}{\sqrt{(mR)^2 + R^2}} - \frac{9}{[(m+1)R]^2} + \frac{4}{[(m+2)R]^2 + R^2}\cdot\frac{(m+2)R}{\sqrt{[(m+2)R]^2 + R^2}}\} \qquad (EQ.-I-05)$$

In the above equation, the first term inside the bracket is for the repellent force from the 4 electrons in plane 2, the second term is for the attracting force from the 9 protons in the nucleus, and the third term is for the repellent force from the 4 electrons in plane 3. Plane 2 and plane 3 are both part of the second layer in which 8 electrons stay.

$$F_{tot} = Kq^2\left\{\frac{4}{R^2}\cdot\frac{m}{(m^2+1)^{3/2}} - \frac{9}{[(m+1)R]^2} + \frac{4}{R^2}\cdot\frac{m+2}{[(m+2)^2+1]^{3/2}}\right\} \quad (EQ.-I-06)$$

When *m* is reasonably large, from Eq.-I-06 we can have

$$F_{tot} = Kq^2\left\{\frac{4}{(mR)^2} - \frac{9}{(mR)^2} + \frac{4}{(mR)^2}\right\} = -\frac{Kq^2}{(mR)^2} \qquad (EQ.-I-07)$$

What $EQ-I-07$ shows is a situation compatible to the treatment of what Eq. 05 expresses: the Coulomb force between one electron and one proton.

When *m* is small, such as m=0.5, from Eq.-I-06 we have

$$F_{tot} = Kq^2\left\{\frac{4}{R^2}\cdot\frac{0.5}{(0.25+1)^{3/2}} - \frac{9}{[1.5R]^2} + \frac{4}{R^2}\cdot\frac{0.5+2}{(2.5^2+1)^{3/2}}\right\} = -\frac{2.05Kq^2}{R^2} \qquad (EQ.-I-08)$$

At the first glance, between $EQ.-I-07$ and $EQ.-I-08$, F_{tot} seemingly appears with a bigger absolute value with a smaller *m*. However, we must notice that the bigger $|-2.05|$ value in $EQ.-I-08$ is contributed by 9 protons; the convenience given to the calculation as if there is only 1 (=9-8) proton exerting coulomb force on one electron can no longer be applied.

Taking the average of the F_{tot} in $EQ.-I-08$ over 9 protons, we have

$$F_{tot,ave} = -\frac{2.05Kq^2}{R^2} \div 9$$

$$= -\frac{0.228Kq^2}{R^2} \qquad (EQ.-I-09)$$

$F_{tot,ave}$ above is quite smaller than $F_e = -k\frac{q\times q}{r^2}$ shown in Eq. 05, where the force is truly contributed by one electron and one proton. Contrasting to the electrical value shown by $EQ-I-09$ at where the most remote electron locates, the Aether's out-pushing force is genuinely caused by 11 protons. If these protons have separated by a significant distance from each other, such an out-pushing force acting on the most remote electron can be easily proven as 11 times strong as 1 of them would cause—while what is contributed regarding the Aether pressure by the 12 neutrons is not even yet mentioned.

According to all up-today pictures that this author can find from authoritative documents, nuclei are shown as aggregates of neutrons and protons closely compacted together with skin contact; no distinctive space is shown between nucleons. However, such presentation of skin contact should be contradicted by the mass density of neutron stars. The mass of a neutron is $1.68\text{x}10^{-27}$ kg, and the densest neutron star found so far has a density of $5.9 \text{ x } 10^{17}$ kg/m^3. That means the average volume occupied by a neutron in the star has a linear dimension of $3 \text{ x } 10^{-13}$ m, a dimension that is at least 100 folds bigger than a nucleus that today's nuclear science literatures commonly speculate today. If gap must be found between all particles comprising a huge physical body like a neutron star, then, gap must also exist between all nucleons within a physical body as small as a nucleus found on Earth. Then, gap must also have higher chance to exist between all nucleons in the sodium nucleus and therefore, the Aether pressure at a large distance from the nucleus can be a simple sum of the pressure caused by each of these nucleons.

Experiencing smaller Coulomb force coming from the nucleus but far bigger out-pushing force caused by 11 protons (plus 12 neutrons, too), the most remote electron would have high tendence to locate itself far away from the rest of the atom. It is particularly so for electrons that belong to the atoms forming the outmost surface of a material body.

Appendix II

—Floating Force Exerted on An Electron—

Refer to Fig-II-01. Because the omnipresence of Aether in the universe [2], it could only be natural that an electron bounded by a nucleus in an atom is inevitably immersed in such fluid. The broken line "surface" in Fig-II-0 1does not mean a distinctive physical border line but only helps to indicate that, in space beyond a certain distance from any material body, this fluid would manifest its existence with intrinsic pressure P_o everywhere. The material body in our concern and is herein referred to is the nucleus in an atom.

If we assume the electron takes a spherical shape, the total force received from the Aether by the lower hemispheres (in black) of this electron sphere is pointing up. We note it as F_{up}. Likewise, the upper hemisphere (in blue) also receives a force from the Aether, but this force is pointing down. We note it as F_{down}.

At a randomly chosen point D on the lower hemisphere, let the pressure found there be P_D. There we also find an infinitesimally small strip (in gray) along the peripheral of the small circle defined by point D and this small circle is parallel to the large circle MN. The area *ds* of this strip can be found in the following:

$$ds = 2\pi r \cdot \Delta l$$
$$= 2\pi R \cos\theta \cdot R d\theta \quad (Eq - II - 01)$$

The up-pointing force $dF_{D,up}$ received by this strip is therefore

$$dF_{D,up} = (P_D \sin\theta) \cdot ds$$
$$= (P_D \sin\theta) \cdot (2\pi R \cos\theta \cdot R d\theta)$$
$$= 2\pi R^2 P_D \sin\theta \cos\theta \, d\theta \quad (Eq - II - 02)$$

In deriving the Newton's gravitational equation, we take it to be safe to assume that the Aether's intrinsic pressure can be found at any distance that is in the order of $1 \times 10^{-8}\, m$ and beyond away from a nucleus. The intrinsic pressure so found is $1.0 \times 10^{12}\, Kg/cm^2$. So, according to what

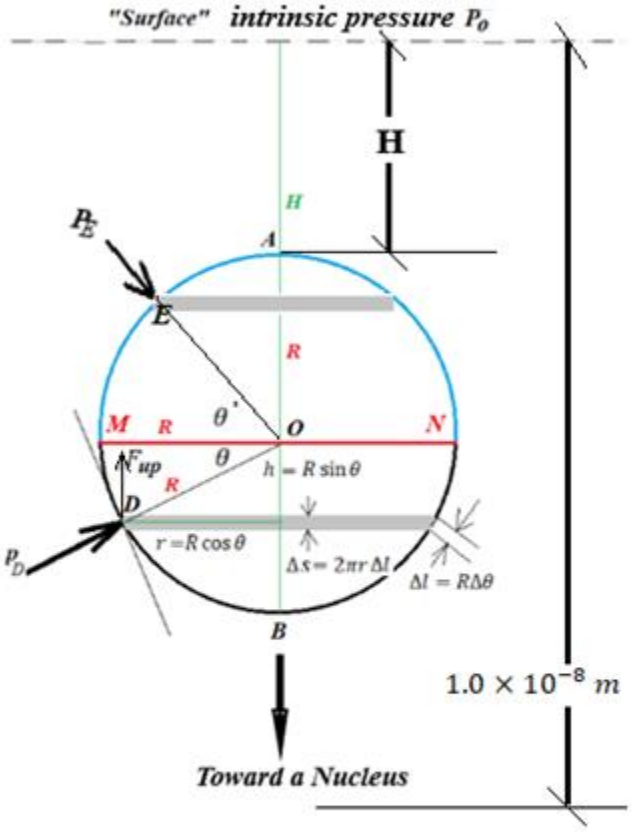

Fig-II-01 Aether Pressure Analysis about an Electron near a Nucleus

is given by Fig. 05 and Eq. 06, P_D in $Eq-II-02$ can be found from the following relationship

$$\frac{P_D}{P_o}=\frac{(1.0\times10^{-8}\,m)^2}{(1.0\times10^{-8}\,m-H-R-h)^2}\qquad(Eq-II-03a)$$

or

$$P_D=\frac{(1.0\times10^{-8}\,m)^2}{(1.0\times10^{-8}\,m-H-R-R\sin\theta)^2}\cdot P_o\qquad(Eq-II-03b)$$

To simplify the equation writing, by making $K_1=(1.0\times10^{-8}\,m)^2$ and $K_2=1.0\times10^{-8}\,m-H-R$, $(Eq-II-02)$ and $(Eq-II-03b)$ together will give us

$$dF_{D,up}=2\pi R^2P_o\frac{K_1}{(K_2-R\sin\theta)^2}\sin\theta\cos\theta\,d\theta\qquad(Eq-II-04)$$

To get the total force of F_{up}, we take integral of both sides of $(Eq-II-04)$ from $-\pi/2$ to 0 then get

$$\begin{aligned}F_{up}&=\int_{-\pi/2}^{0}2\pi R^2P_o\frac{K_1}{(K_2-R\sin\theta)^2}\sin\theta\cos\theta\,d\theta\\&=2\pi P_oK_1\left[\frac{K_2}{-R\sin\theta+K_2}+\ln(-R\sin\theta+K_2)\right]_{-\pi/2}^{0}\\&=2\pi P_oK_1\left\{(1+\ln K_2)-\left[\frac{K_2}{K_2+R}+\ln(K_2+R)\right]\right\}\qquad(Eq-II-05)\end{aligned}$$

For the upper hemisphere, the force exerted on it by the Aether is F_{down}, pointing toward the nucleus. With a similar reasoning but with a force acting on an infinitesimally small strip about a small circle defined by point E that is randomly chosen, the differential force element is

$$\begin{aligned}dF_{E,down}&=(P_D\sin\theta)\cdot\Delta s'\\&=(P_E\sin\theta')\cdot(2\pi R\cos\theta'\cdot Rd\theta')\\&=(P_E\sin\theta')\cdot(2\pi R\cos\theta'\cdot Rd\theta')\\&=2\pi R^2P_E\sin\theta'\cos\theta'\,d\theta'\qquad(Eq-II-06)\end{aligned}$$

Parallel to $(Eq-II-03b)$, we can similarly write an equation for P_E with the following relationship:

$$\frac{P_E}{P_o}=\frac{(1.0\times10^{-8}\,m)^2}{(1.0\times10^{-8}\,m-H-R+h)^2}$$

or

$$P_E = \frac{(1.0 \times 10^{-8}\, m)^2}{(1.0 \times 10^{-8}\, m - H - R + R\sin\theta')^2} \cdot P_o \qquad (Eq - II - 07)$$

We can then have the infinitesimal force element acting on this strip as

$$dF_{D,down} = 2\pi R^2 P_o \frac{K_1}{(K_2 + R\sin\theta')^2} \sin\theta' \cos\theta'\, d\theta' \qquad (Eq - II - 08)$$

Taking integral on both sides of $(Eq - II - 08)$ from 0 to $\pi/2$, we have

$$F_{down} = \int_{\pi/2}^{0} 2\pi R^2 P_o \frac{K_1}{(K_2 + R\sin\theta')^2} \sin\theta' \cos\theta'\, d\theta'$$

$$= 2\pi P_o K_1 \left[\frac{K_2}{R\sin\theta' + K_2} + \ln(R\sin\theta' + K_2)\right]_0^{\pi/2}$$

$$= 2\pi P_o K_1 \left\{\left[\frac{K_2}{R + K_2} + \ln(R + K_2)\right] - (1 + \ln K_2)\right\} \qquad (Eq - II - 09)$$

The net floating force F_{fl} is then

$$F_{fl} = F_{up} - F_{down}$$

$$= 4\pi P_o K_1 \left\{(1 + \ln K_2) - \left[\frac{K_2}{R + K_2} + \ln(K_2 + R)\right]\right\}$$

$$= 4\pi P_o (1.0 \times 10^{-8}\, m)^2 \left(\frac{R}{R + 1.0 \times 10^{-8}\, m - H - R} + \ln\frac{1.0 \times 10^{-8}\, m - H - R}{R + 1.0 \times 10^{-8}\, m - H - R}\right)$$

$$= 4\pi P_o (1.0 \times 10^{-8}\, m)^2 \left[\frac{R}{1.0 \times 10^{-8}\, m - H} + \ln\frac{1.0 \times 10^{-8}\, m - (H + R)}{1.0 \times 10^{-8}\, m - H}\right] \qquad (Eq - II - 10)$$

Since R is the radius of an electron, being extremely small compared to H, and therefore H+R can be taken directly as H. We then can rewrite $(Eq - II - 10)$ as

$$F_{fl} = 4\pi P_o (1.0 \times 10^{-8}\, m)^2 \cdot \frac{R}{1.0 \times 10^{-8}\, m - H}$$

$$= 4\pi \cdot\ 1.0 \times 10^{17} \frac{N}{m^2} \cdot 1.0 \times 10^{-16} m^2 \cdot \frac{R}{1.0 \times 10^{-8}\, m - H}$$

$$= \frac{40\pi R}{1.0 \times 10^{-8}\, m - H} \cdot N \qquad (Eq - II - 11)$$

At the supposed outer edge of a sodium atom, the most remote electron has a distance of $0.227nm$ from the nucleus. This give us $H = 1.0 \times 10^{-8}\, m - 0.227nm$, and $(Eq - II - 11)$ gives us

$$F_{fl} = \frac{40\pi R}{0.227 \times 10^{-9}\, m} \cdot N = 5.53\ \times 10^{11} R\ \cdot N/m \qquad (Eq - II - 12)$$

If we assume the radius of the electron sphere being in the order of $\times 10^{-18} m$, the floating force for the electron is still bigger than the Coulomb force it receives from the nucleus. Therefore, the electron, which can have the freedom of repeating the same movement at frequency of 1×10^{15} times every second and thus generates light, cannot be in the space between atoms, but is pushed to space outside of the entire material body of a chunk.

Appendix III

—Surface Charge Density Per Unit Area of a Sodium plate—

Mass density for sodium is 0.968 gm/cm^3, and atomic weight is 23. So, the volume of one mole of sodium atom is

$$\frac{23\ gm}{0.968\ \mathrm{gm}/_{cm^3}} = 23.76\ cm^3 \qquad (Eq.III - 01)$$

If such a volume is shaped as a cube, each edge of this cube would be $2.87cm$, and the area A of each face of this cube would be

$$A = (2.87cm)^2 = 8.24\ cm^2 \qquad (Eq.III - 02)$$

One mole of sodium has 6.022×10^{23} atoms and therefore each atom has a volume of

$$\frac{23.76\ cm^3}{6.022 \times 10^{23}} = 3.95 \times 10^{-23} cm^3$$

$$= 3.95 \times 10^{-27} m^3 \qquad (Eq.III - 03)$$

If each of this little volume is a cube, its edge would be $1.58 \times 10^{-9} m$ and each face has an area of

$$A' = \left(1.58 \times 10^{-9} m\right)^2 = 2.5 \times 10^{-18} m^2 \qquad (Eq.III - 04)$$

Suppose the sodium atoms align themselves very orderly and tightly in the surface shown by Eq-III-02, the number of sodium atoms filled in A would be

$$\frac{8.24cm^2}{2.5\times10^{-18}m^2}=3.3\times10^{14} \qquad (Eq.III-05)$$

If each atom lying in this surface loses one electron, the area density of charge of this area would be

$$\theta=+\frac{3.3\times10^{14}q}{A'}=+\frac{3.3\times10^{14}\cdot1.6\times10^{-19}C}{2.5\times10^{-18}m^2}=+2.11\times10^{13}C/m^2 \qquad (Eq.III-06)$$

Reference

[1] Relativity is self-refuted, c=0, —So "Proven" by Special Relativity, by *Cameron Rebigsol* ,

https://vixra.org/pdf/1912.0453v1.pdf

[2] **First Evidence of Aether**—Newton's gravitational Law, *Cameron Rebigsol*, https://vixra.org/pdf/2003.0452v1.pdf

[3] **Second Evidence of Aether**—Ives-Stilwell Experiment, *Cameron Rebigsol*, https://vixra.org/pdf/2005.0091v3.pdf

[4] https://en.wikipedia.org/wiki/Photoelectric_effect

[5] https://physicsworld.com/a/how-long-does-the-photoelectric-effect-take/

A Parameter-Driven Approach to Synchronize Single and Double Pendulums Using the Kuramoto Model for Real-World Applications

Kaival Shah*

Abstract

This paper investigates the relationship between single and double pendulum synchronization and real-world synchronization. The Kuramoto model was applied to couple single pendulums and the results were analyzed for implementing double pendulum synchronization. A differential equation approach was utilized to model N double pendulums, and an ordinary differential equation solver was implemented in Python. Double pendulum oscillations were modeled using the Lagrangian equations of motion due to the constraint independent benefits. Investigation outcomes were utilized to explain synchronization phenomena in real-world dynamical systems: lockstep, Galilean moons, Centaurus A, Belousov-Zhabotinsky reaction. Single pendulum synchronization was achieved with sufficient coupling power K. Double pendulum synchronization was achieved with a sufficiently small initial displacement from equilibrium, stable constants for mass and length, and sufficient coupling strength K. The results yield the possibility of phase-shifted synchronization for chaotic systems contingent upon the system's ability to overcome state-dependent chaos.

1 Introduction

Synchronization is a phenomenon observed throughout nature in fields such as biology, chemistry, astronomy, electronics, and physics. Studying synchronization in chaotic systems or simplifying system variabilities yields a greater understanding or potential generalization of unsolved problems. In physics, the classical example of synchronization studied by Dutch mathematician Christiaan Huygens and Dutch physicist Balthasar van der Pol is the oscillatory behavior exhibited by a set of pendulums mechanically connected by a spring or balance beam. The physical connection between the oscillators enables communication through vibrations. As these vibrations interpose, dominant waves persist and guide the system. Other instances of synchronization in physics include superconducting Josephson junctions, microwave oscillators, side-by-side organ pipes, and electrical generator frequencies. Japanese Physicist Yoshiki Kuramoto formulated the Kuramoto model (Section 4), a mathematical representation of synchronous behavior for a system consisting of N general oscillators. In addition to synchrony in stable systems, more relevant examples involve achieving synchrony in chaotic systems. The double pendulum, studied by Swiss mathematician Daniel Bernoulli, is chaotic in nature. Chaotic systems are difficult to stabilize, especially systems with large initial displacements from equilibrium. Subtle deviations grow over time and exit simple mechanics. As a result of managing constraints, modeling double pendulum behavior with ordinary Newtonian mechanics is difficult. Alternatively, the Lagrangian formulation is useful for constraint-independent models, involving the kinetic energy and potential energy of the system. Due to high variability in physics models, these formulations yield a new dimension of useful modeling methods. A computational approach, involving differential equations and numerical integration, is necessary when modeling chaotic systems due to the high process time and inefficiency in analytical solutions.

*Advised by Dr. Andy Haas, Professor of Physics at New York University.

2 Research Questions

1. How do communicating single pendulums synchronize? What parameters affect how quickly they synchronize?
2. Do communicating double pendulums synchronize? What parameters affect their synchrony?
3. What do synchronization results imply for real-world phenomena?

3 Methods

Two computational approaches are taken to model single pendulum synchronization and double pendulum synchronization. Computational approach 1 is preferred for modeling single pendulum synchronization due to the expected behavior of the underlying system. Computational approach 2 is utilized for single pendulum synchronization due to scalability purposes. Both methods achieve the same outcome. Method 1 involves classical modeling whereas method 2 involves numerical integration of differential equations for state position estimation. This method is then scaled to double pendulum synchronization, which also relies on a differential approach.

3.1 System Initialization

The single pendulum model and double pendulum model rely on arbitrarily defined initial parameters. Specific to single pendulum synchronization, initial conditions are defined randomly, which helps reveal the significance of synchronization. Double pendulum synchronization relies on arbitrarily distinct values such that state-dependent chaos is introduced and events of synchronization are plausible.

3.2 System Variation

Computational approach 2 is best suited for parameter variation. Parameter variation involves deviating individual parameters and analyzing the effects of those deviations on events of synchronization. During parameter deviation, the remaining system constraints are fixed. System variation is particularly important for double pendulum synchronization because subtle deviations generate drastic outcomes. These subtle deviations often vary system synchronization categorization.

4 The Kuramoto Model

Eq. (1) presents the Kuramoto model, where ω_i represents the intrinsic frequency, K represents the coupling strength of the system, and N represents the number of pendulums in the system. $\frac{1}{N}$ is a normalization factor. The method in which each oscillator interacts is sinusoidal. The model compares the θ of two distinct oscillators N times such that, for each iteration, the coupling function defined by $\sin(\theta_j - \theta_i)$ will either positively or negatively contribute to the ith oscillator's intrinsic frequency ω_i.

$$\frac{d\theta_i}{dt} = \omega_i + \frac{K}{N}\sum_{j=1}^{N}\sin(\theta_j - \theta_i), \qquad i = 1 \dots N \tag{1}$$

If, for instance, the intrinsic frequency ω_i for each oscillator is widely spread apart and the coupling strength K is too weak to impact the intrinsic frequency of each oscillator, the system will either not synchronize or take more time to synchronize. Three categorizations of synchronized oscillators exist: nil phase-locking, partial phase-locking, and full phase-locking [GHW17]. This paper attempts to achieve full phase-locking in orderly and chaotic systems.

5 Simulating Single Pendulum Synchronization

5.1 Parameters Affecting the Communication Between Synchronizing Single Pendulums

The Kuramoto model (Section 4) can be used to simulate a system of N coupling pendulums with a coupling strength K. The ability of a given system to synchronize depends on the `x_limit`. With an insufficient `x-limit`, the system may not synchronize in the iteration time provided. As a result, a sufficiently large `x-limit` is provided to analyze the affects of variations in the values of parameters. Across simulations, `x-limit` is held constant for synchronization investigative purposes.

5.2 Computational Approach 1: Single Pendulum Synchronization

In the `computations` function presented below, the phase difference for N single pendulums is computed and utilized to regulate the system's ordinary oscillatory behavior. The `computations` function works by computing the phase difference between oscillators, and conducting coupling at the micro-scale accordingly. The full source code is given by [Sha22].

```
def single_pendulum_computations(t):
    for oscillator_i in range(0, number_of_pendulums):
        error = 0
        for oscillator_j in range(0, number_of_pendulums):
            if oscillator_j != oscillator_i:
                error += math.sin(
                    current_positions[oscillator_j] - current_positions[oscillator_i]
                )
        new_positions[oscillator_i] = (
            current_positions[oscillator_i]
            + (coupling_strength_K * error) / number_of_pendulums
        )
        updated_positions.append(new_positions[oscillator_i])
        position_axis[oscillator_i].append(math.sin(t + new_positions[oscillator_i]))
```

A model is created with $N = 70$ single pendulums, coupling strength $K = 0.07$, and standard deviation threshold $\sigma_T = 0.008$. N and K are arbitrarily determined, and σ_T is determined experimentally. A substantially large σ_T will undermine events of synchronization and a substantially small σ_T will rarely isolate events of synchronization. σ_T must be held constant to adequately analyze events of synchronization because a state-dependent σ_T will hinder the deterministic property of modeled synchronization.

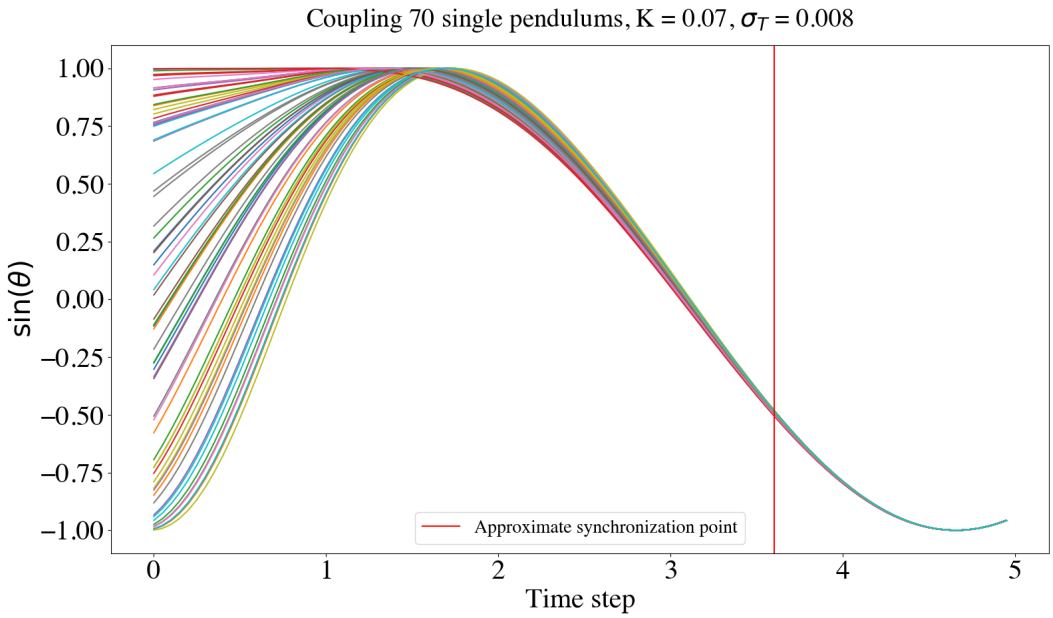

Figure 1: $\sin(\theta)$ vs. Time step.

A more systematic approach is taken: incrementing a parameter and determining the approximate synchronization time.

5.2.1 Approximate Synchronization Point *versus* K

With a fixed σ_T, varying the coupling strength K inversely affects the approximate synchronization time. σ_T is used because complete synchrony is unachievable. Approximate synchrony is determined when $\sigma_i \leq \sigma_T$. Varying K enables the examination of optimal synchronization conditions.

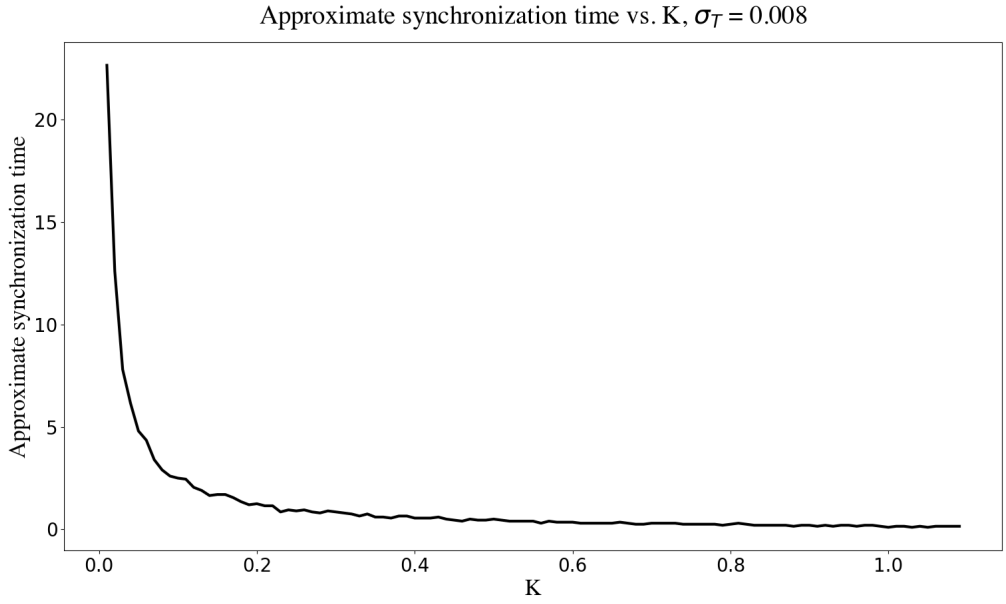

Figure 2: Approximate synchronization time vs. K.

5.3 Computational Approach 2: Single Pendulum Synchronization

Ordinary differential equations and the `odeint` integrator from `SciPy` yield a second method to model single pendulum synchronization [Oli21] [VGO+20]. The initial angular velocity ω of $N = 2$ single pendulums is variable, a method which scales from one to two degrees of freedom for double pendulum synchronization (Section 6). Rather than relying merely on the initial angular position of the the single pendulums, this approach welcomes further variability: initial angular position and initial angular velocity. The single pendulum can be represented by the non-linear differential equation $\ddot{\theta} = -\frac{g}{L}\sin(\theta)$.

To analyze the system's coupling ability, both single pendulums are defined with different initial conditions, but the coupling strength is held constant at $K = 0.3$.

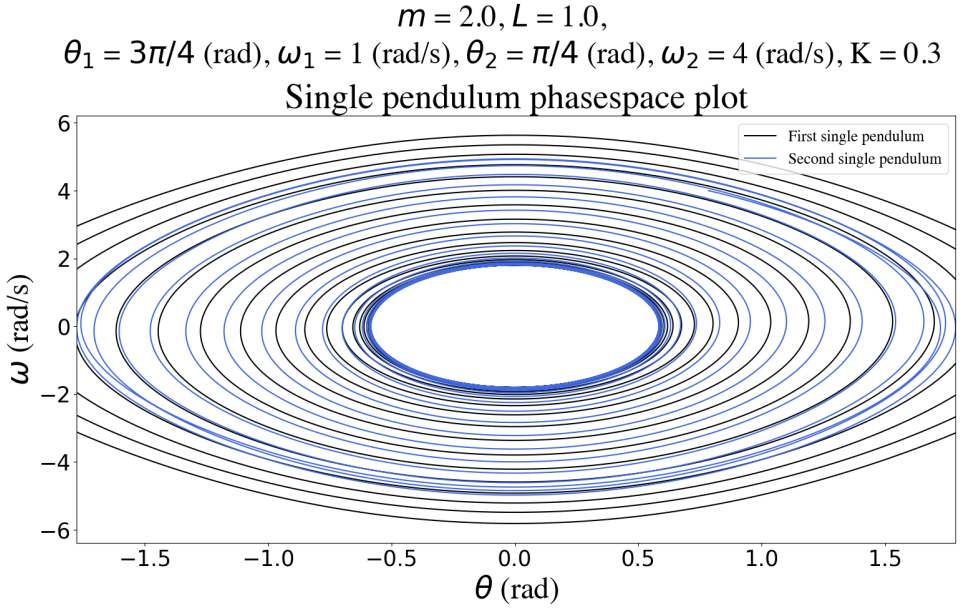

Figure 3: ω_i $(\frac{\text{rad}}{\text{s}})$ vs. θ_i (rad).

6 Simulating Double Pendulum Synchronization

Table 1: Variables

Variable Name	Description
g	Acceleration due to gravity
ω	Angular velocity
L_1	First rod length
θ_1	First rod angular displacement
m_1	First mass
L_2	Second rod length
θ_2	Second rod angular displacement
m_2	Second mass

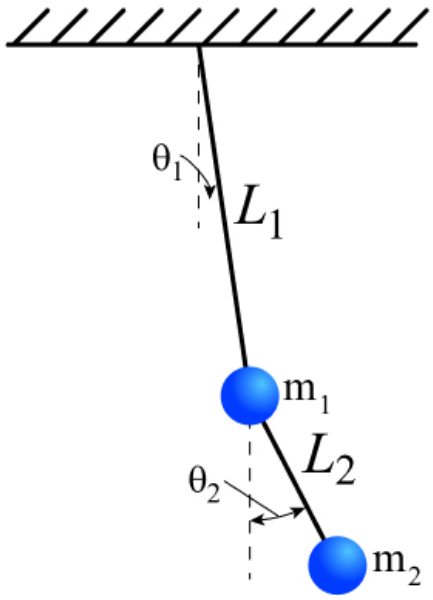

Figure 4: Double pendulum setup [Jab08].

The Lagrangian equations of motion (2, 3, 4, 5) are used to simulate the motion of a double pendulum.

$$\omega_1 = \dot{\theta}_1 \tag{2}$$

$$\omega_2 = \dot{\theta}_2 \tag{3}$$

$$\dot{\omega}_1 = \frac{1}{L_1((\cos(\theta_1 - \theta_2))^2 m_2 - m_1 - m_2)} \Big[L_1 m_2 \cos(\theta_1 - \theta_2) \sin(\theta_1 - \theta_2) \omega_1^2 + L_2 m_2 \sin(\theta_1 - \theta_2) \omega_2^2 - m_2 g \cos(\theta_1 - \theta_2) \sin\theta_2 + (m_1 + m_2) g \sin\theta_1 \Big] \tag{4}$$

$$\dot{\omega}_2 = \frac{1}{L_2((\cos(\theta_1 - \theta_2))^2 m_2 - m_1 - m_2)} \Big[L_2 m_2 \cos(\theta_1 - \theta_2) \sin(\theta_1 - \theta_2) \omega_2^2 + L_1 (m_1 + m_2) \sin(\theta_1 - \theta_2) \omega_1^2 + (m_1 + m_2) g \sin\theta_1 \cos(\theta_1 - \theta_2) - (m_1 + m_2) g \sin\theta_2 \Big] \tag{5}$$

The equations are written as four first-order differential equations because the `odeint` integrator from `scipy` supports integration for first-order differential equations [Oli21] [VGO+20].

6.1 Computational Approach 2: Double Pendulum Synchronization

The code below represents the synchronization behavior of two double pendulums, each with four individually initialized conditions: θ_1, ω_1, θ_2, ω_2. These conditions represent the motion of each double pendulum at time $t = 0$. The other parameters responsible for the behavior of each double pendulum are the mass and length: m_1, m_2, L_1, L_2. To analyze the impact of the Kuramoto model on N double pendulums, the lengths L_1, L_2 and the masses m_1, m_2 are kept constant. Similar to the single pendulum model, a coupling strength K is used for the double pendulum simulation. The full source code is given by [Sha22].

Christiaan Huygens discovered that two swinging single pendulums connected by a beam communicate with one another via their physical connection to the beam [PRONA16]. The way Huygens setup his single pendulum experiment is replicated in this paper for double pendulums; however, the Kuramoto model will be used instead of conducting double pendulum communication via a beam. Specifically, θ_1 for all N double pendulums will couple with each other and θ_2 will not be directly impacted by the Kuramoto model. This is because, in the classical example that this model represents, only the primary rod (m_1, L_1, θ_1, ω_1) is influenced by the vibration signals of the beam. Thus, the second half of each double pendulum (m_2, L_2, θ_2, ω_2) will change depending on the state of the first half of the double pendulum, which allows the system to maintain its chaotic attributes.

```
def double_pendulum_computations(z, time, L1_1,
                                 L2_1, L1_2, L2_2, m1_1, m2_1,
                                 m1_2, m2_2, g, coupling_strength_K,
                                 number_of_pendulums):
    pendulum_values = []
    return_values = []
    pendulum_values.extend(z)
    for oscillator_i in range(0, number_of_pendulums):
        error = 0
        for oscillator_j in range(0, number_of_pendulums):
            if oscillator_i != oscillator_j:
                error += np.sin(pendulum_values[oscillator_j * 4]
                    - pendulum_values[oscillator_i * 4])
        pendulum_values[oscillator_i * 4 + 1] += ((coupling_strength_K * error) /
                                                  number_of_pendulums)
    for oscillator_i in range(0, number_of_pendulums):
        L1 = L1_1 if oscillator_i == 0 else L1_2
        L2 = L2_1 if oscillator_i == 0 else L2_2
        m1 = m1_1 if oscillator_i == 0 else m1_2
        m2 = m2_1 if oscillator_i == 0 else m2_2
        theta1, w1, theta2, w2 = pendulum_values[oscillator_i * 4 : oscillator_i * 4 + 4]
        xi = np.cos(theta1 - theta2) ** 2 * m2 - m1 - m2
        w1dot = (L1 * m2 * np.cos(theta1 - theta2) * np.sin(theta1 - theta2) * w1**2
            + L2 * m2 * np.sin(theta1 - theta2) * w2**2
            - m2 * g * np.cos(theta1 - theta2) * np.sin(theta2)
            + (m1 + m2) * g * np.sin(theta1)) / (L1 * xi)
        w2dot = -(L2 * m2 * np.cos(theta1 - theta2) * np.sin(theta1 - theta2) * w2**2
            + L1 * (m1 + m2) * np.sin(theta1 - theta2) * w1**2
            + (m1 + m2) * g * np.sin(theta1) * np.cos(theta1 - theta2)
            - (m1 + m2) * g * np.sin(theta2)) / (L2 * xi)
        return_values.extend([w1, w1dot, w2, w2dot])
    return return_values
```

6.2 Computational Analysis

A double pendulum is chaotic in nature and a resulting factor of this chaotic motion is that small changes in initial conditions can lead to drastic changes in the overall motion of the system. This phenomenon is known as the butterfly effect, and a simulation of the butterfly effect is given by [Gus21].

Due to the chaotic nature of a double pendulum, what follows is the impact of changing specific parameters on the system's ability to synchronize. To simplify the results, $N = 2$ double pendulums are used. A graph comparing the difference between θ_1 for both double pendulums and a second graph comparing the difference between θ_2 for both double pendulums are constructed.

6.2.1 The Control

For the control, two double pendulums are initialized with slightly different conditions to ensure synchronization. The graph on the left represents the ability of θ_1 to synchronize for both double pendulums. The graph on the right represents the ability of θ_2 to synchronize for both double pendulums.

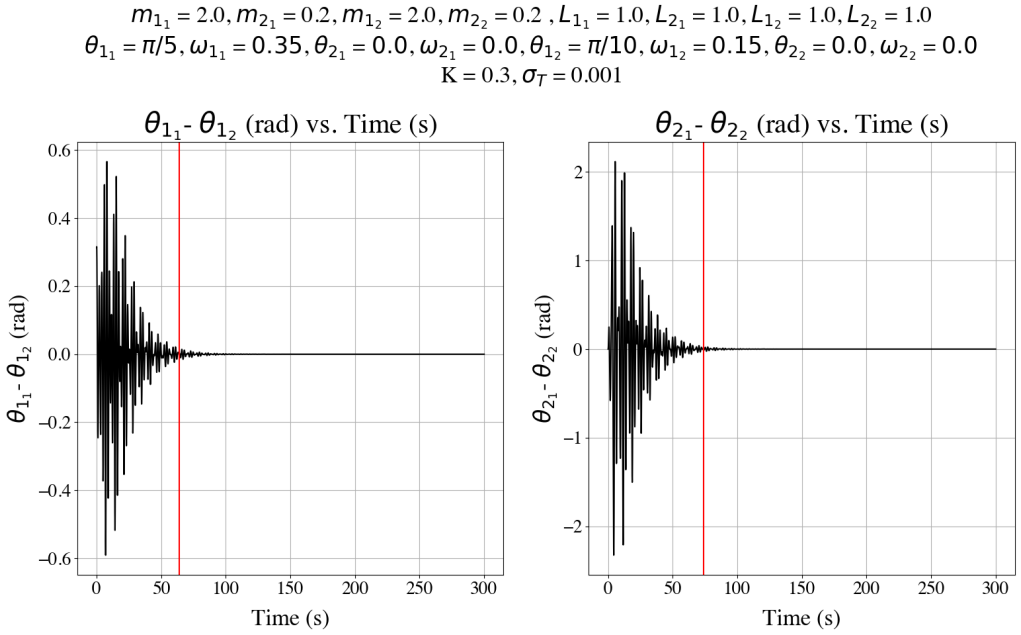

Figure 5: Both pendulums are able to synchronize their θ_1 and θ_2 with some phase difference. At the start of the system, both double pendulums exhibit the inherent dynamics of a chaotic system. The coupling soon reduces this chaotic motion.

For each system, an additional pair of graphs depicting double pendulum position variability is provided. The graph to the left represents the raw variability and the graph to the right represents a logarithmic transformation of the double pendulum position variability. Together, both graphs reveal the categorization of synchronization.

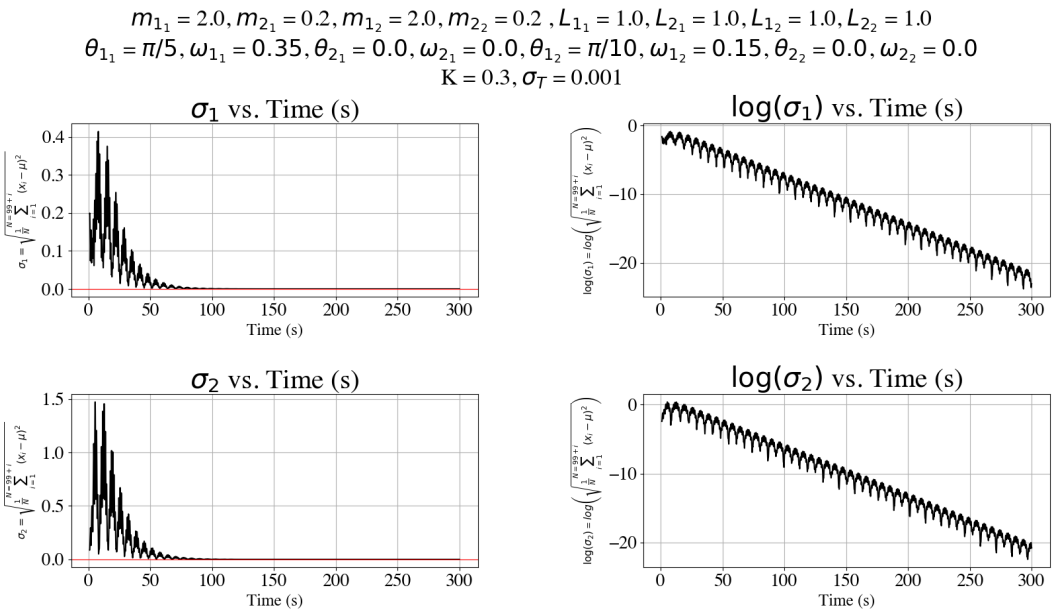

Figure 6: σ_i vs. Time (s) and $\log(\sigma_i)$ vs. Time (s). The variation between the positions of the double pendulums significantly decreases within the first 100 seconds as a result of coupling.

Included below (Section 6.2.2) are the notable results for double pendulum synchronization as changes are made to deviate from the control. Changed parameters include mass, length, angle, and angular velocity. Further experimentation with the double pendulum source code [Sha22] is encouraged.

6.2.2 Deviating from the Control

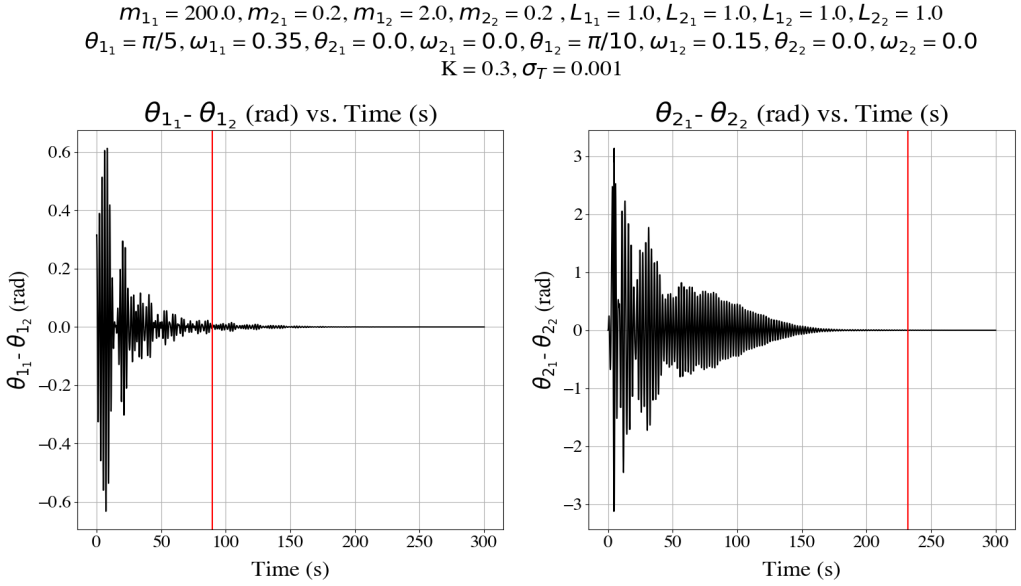

Figure 7: After increasing the m_{1_1} by a factor of 100, θ_{1_1} and θ_{1_2} are still able to synchronize with a phase difference. Although θ_{2_1} and θ_{2_2} are also able to synchronize, it takes longer because the Kuramoto model is only directly coupling θ_1 of both double pendulums.

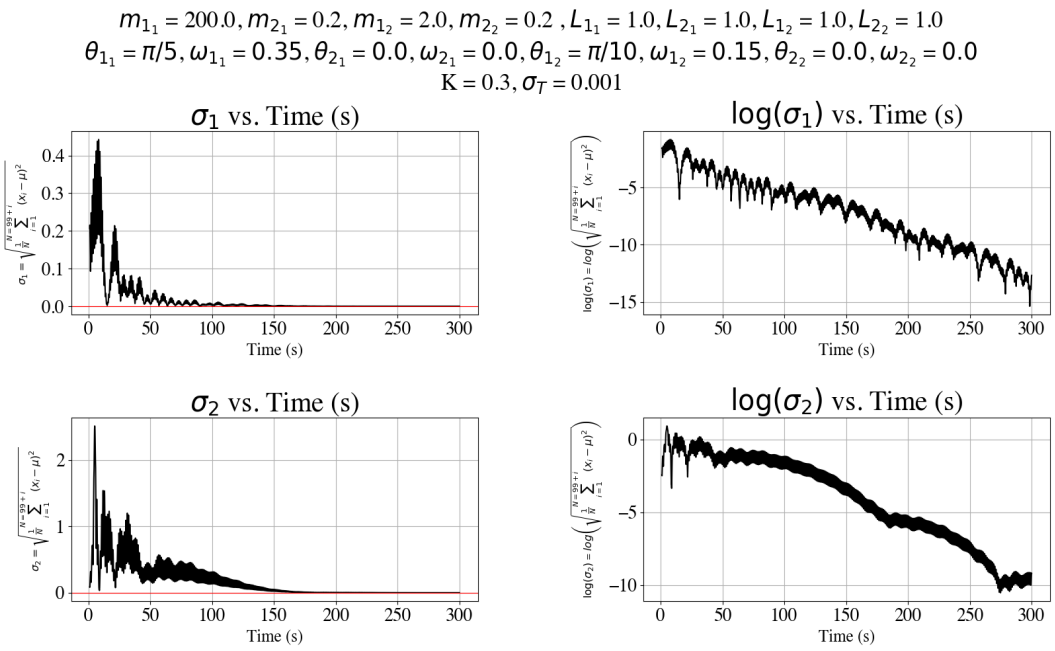

Figure 8: σ_i vs. Time (s) and $\log(\sigma_i)$ vs. Time (s).

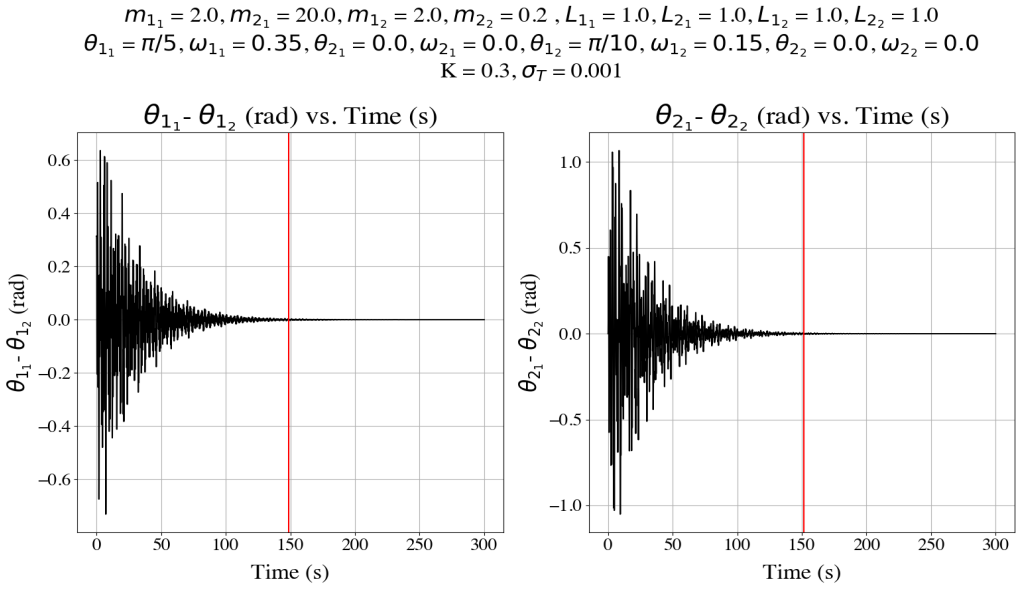

Figure 9: After increasing m_{2_1} by a factor of 100, θ_{1_1} and θ_{2_1} are able to couple and θ_{2_1} and θ_{2_2} are able to couple. Coupling takes place earlier for θ_2 and both synchronization times are closer to one another than the former. Hence, increasing m_{2_1} impacts the system differently than increasing m_{1_1}.

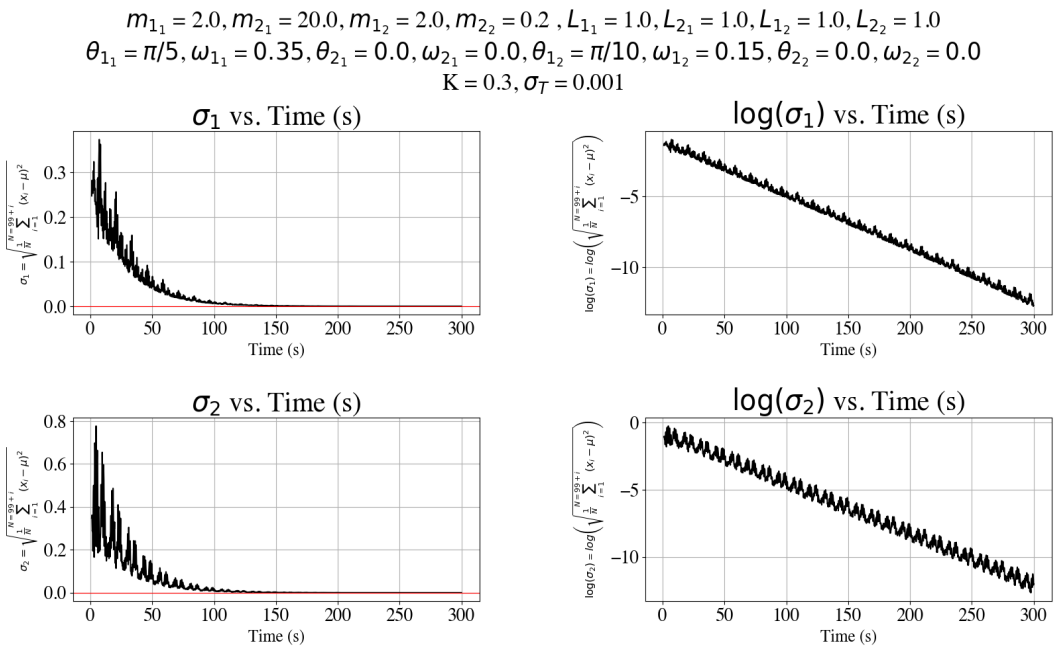

Figure 10: σ_i vs. Time (s) and $\log(\sigma_i)$ vs. Time (s).

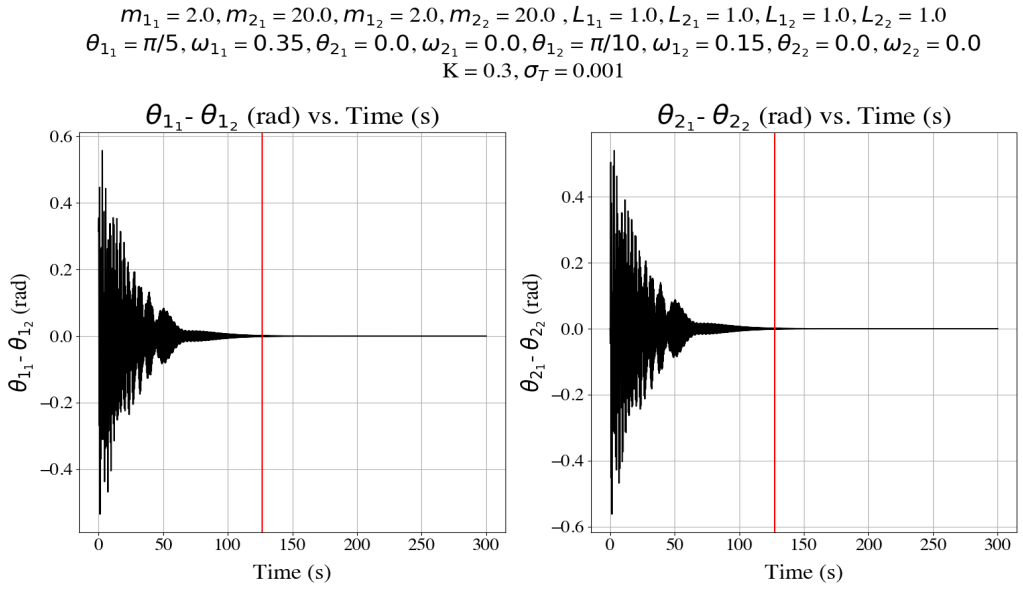

Figure 11: After increasing m_2 for both double pendulums by a factor of 100, θ_1 and θ_2 synchronize faster.

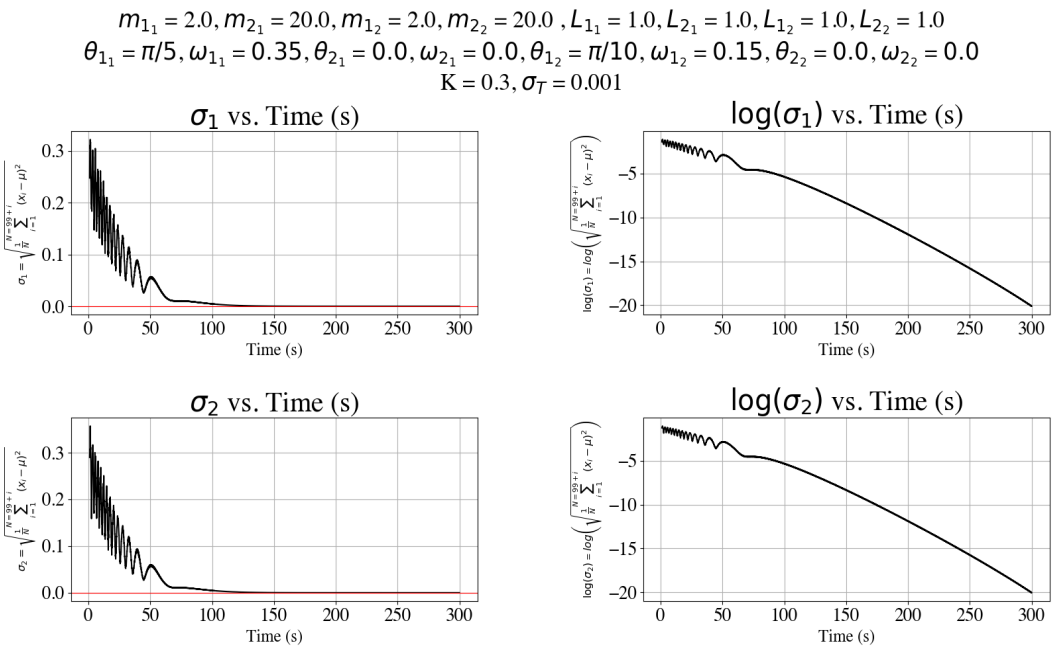

Figure 12: σ_i vs. Time (s) and $\log(\sigma_i)$ vs. Time (s).

Other results arise when varying θ_1, ω_1, θ_2, and ω_2 for each of N double pendulums.

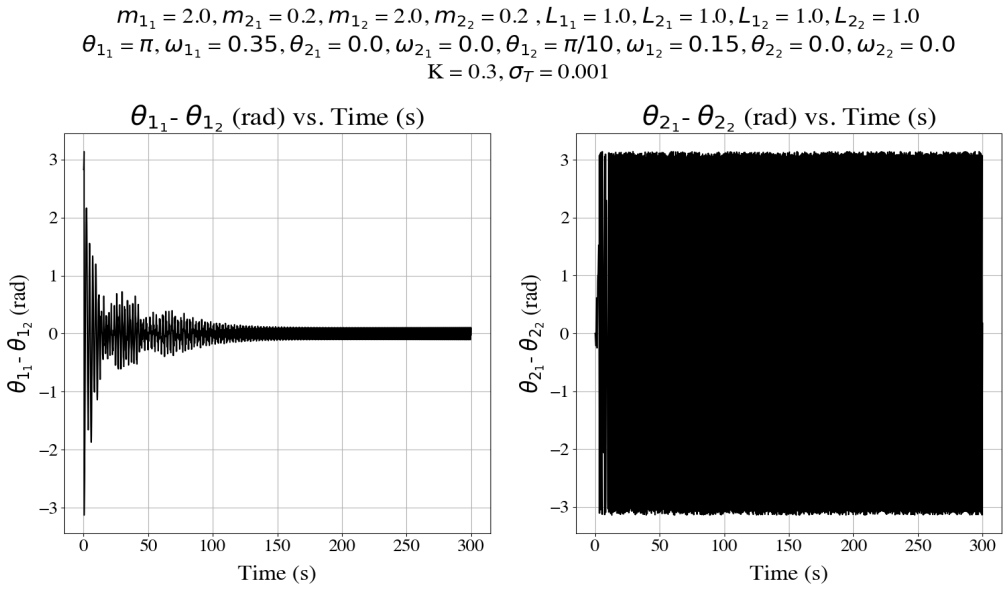

Figure 13: As θ_{1_1} starts at π instead of $\frac{\pi}{5}$, the first double pendulum begins at a location further away from equilibrium. This results in uncontrollable chaotic swinging, which prevents θ_1 and θ_2 for both double pendulums from synchronizing.

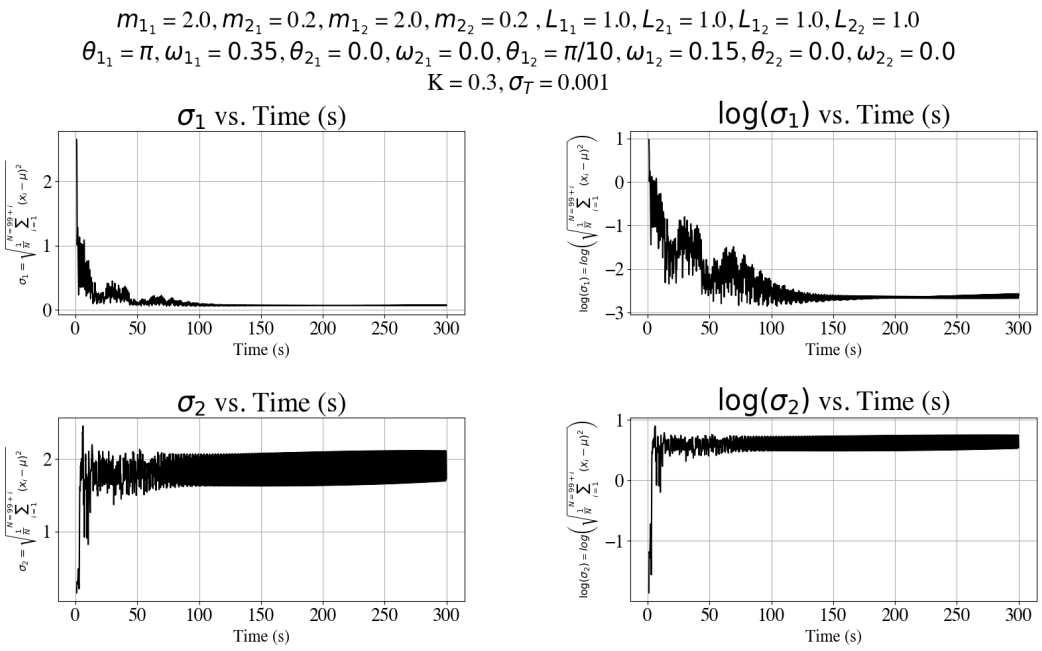

Figure 14: σ_i vs. Time (s) and $\log(\sigma_i)$ vs. Time (s).

One way to attempt to return to synchrony is by increasing the angular velocity of θ_{1_1}. In the previous example, $\omega_{1_1} = 0.35$. If we set $\omega_{1_1} = 2.35$, the increase in angular velocity will allow the first double pendulum to return to synchrony.

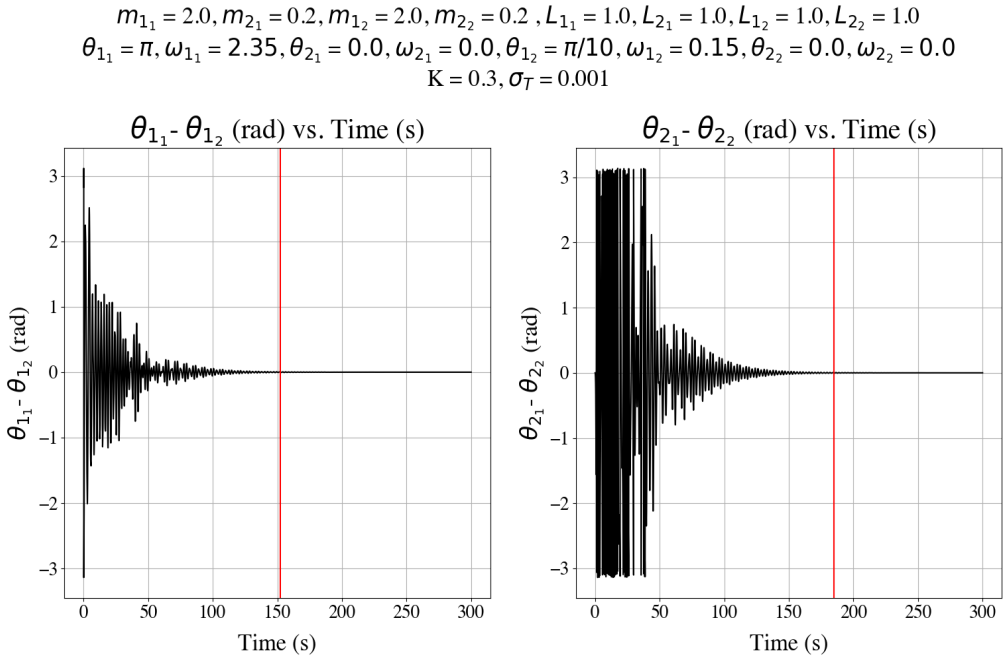

Figure 15: Both double pendulums take more time to approach synchrony. Approaching synchrony in this situation signifies that increasing the angular velocity compensates for an increase in the double pendulum's initial disequilibrium.

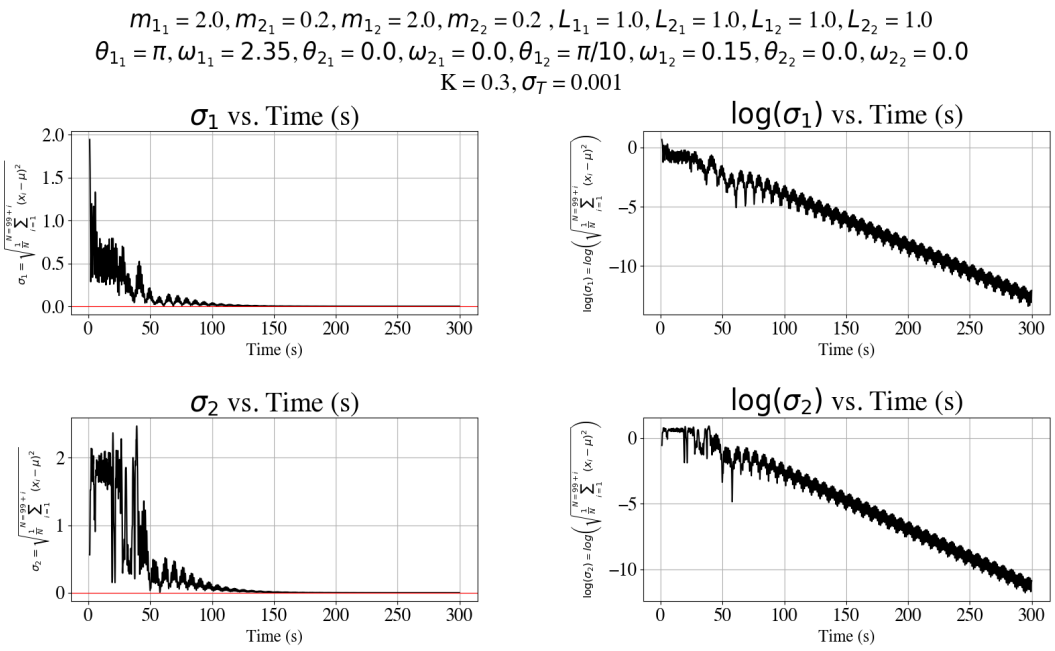

Figure 16: σ_i vs. Time (s) and $\log(\sigma_i)$ vs. Time (s).

6.3 Synchronization Time *versus* Increment

Incrementing a parameter and approximating the synchronization time yields a graph comparing the changing parameter to the approximate synchronization time given σ_T.

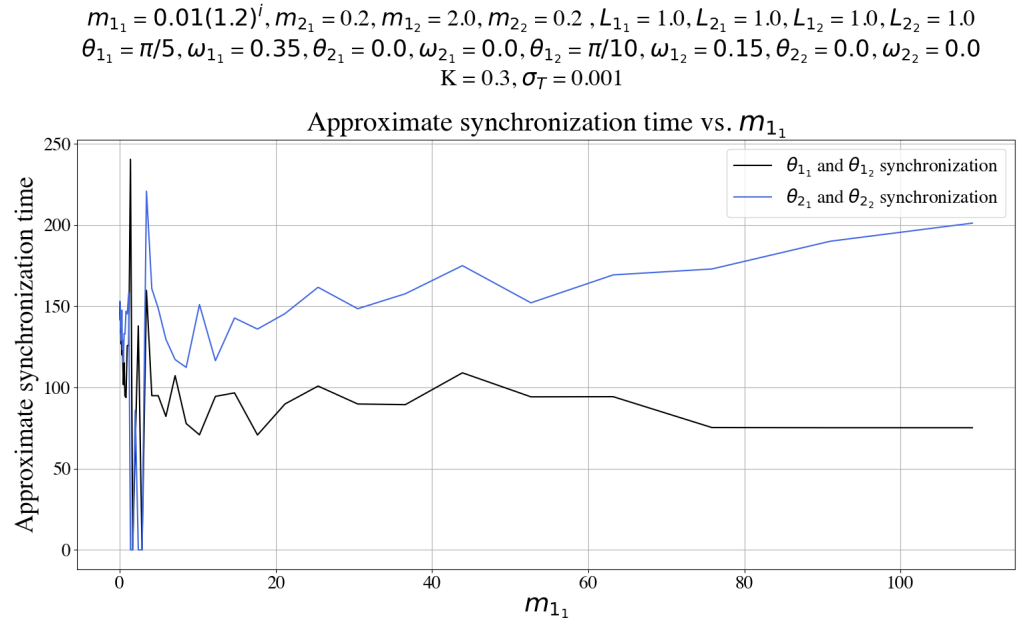

Figure 17: There exists a weak relationship between the value of m_{1_1} and the approximate synchronization time.

$m_{1_1} = 2.0, m_{2_1} = 0.2, m_{1_2} = 2.0, m_{2_2} = 0.2\ , L_{1_1} = 1.0, L_{2_1} = 1.0, L_{1_2} = 1.0, L_{2_2} = 1.0$
$\theta_{1_1} = \pi/5, \omega_{1_1} = 0.35, \theta_{2_1} = 0.0, \omega_{2_1} = 0.0, \theta_{1_2} = \pi/10, \omega_{1_2} = 0.15, \theta_{2_2} = 0.0, \omega_{2_2} = 0.0$
$\mathrm{K} = 0.01 \ldots 10.0, \sigma_T = 0.001$

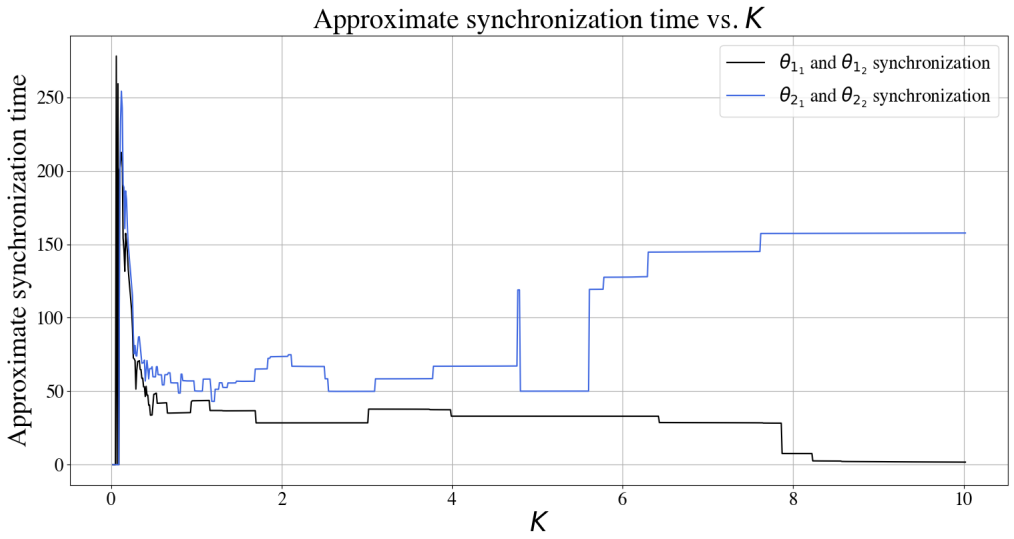

Figure 18: As the coupling strength K increases, the time it takes for the system to synchronize significantly decreases for θ_{1_1} and θ_{1_2}. Unlike single pendulum synchronization (Section 5), the chaotic nature of a double pendulum system prevents any predictable inverse relationship. Interestingly, as K increases, the synchronization time increases for θ_{2_1} and θ_{2_2} after initially decreasing.

7 Applications to Real-World Phenomena

In June 2000, when the London Millennium Footbridge first opened to the public, around 90,000 people walked on the bridge. Not long after the bridge was opened, however, people began to realize a large lateral swaying motion. The bridge was closed a few days later. Architects attributed this unusual lateral behavior to the positive-feedback loop created by the bridge's structural resonance. It is a human tendency to move left and right when taking a step forward. Although the pattern of steps taken by a group of individuals is inherently random, the subtle lateral movement of the bridge influenced individuals into lockstep with one another. As time passed, this lockstep further propagated the bridge's lateral movement. It was later identified that the bridge's movement acted as an external driving force for the system and coupled the steps of individuals walking on the bridge. This is similar to the single pendulum model because the way people take steps varies from person to person, similar to the intrinsic frequency of each pendulum. The coupling done by the bridge is similar to the contributions made by the Kuramoto model in the single pendulum simulation.

Figure 19: The London Millennium Footbridge [LRP07].

Another example of synchronization in nature is found in astronomy. Understanding the underlying nature of synchronization phenomena can help scientists further their knowledge about abstract concepts. In particular, Jupiter's Io, Europa, and Ganymede moons have a special interaction known as orbital resonance. In this case, the orbital resonance between Io, Europa, and Ganymede creates a 4:2:1 orbital ratio where the moons repetitively meet each other in a self-correcting manner. This situation is only possible if the gravitational forces are stable enough for repetition and the system is able to self-correct as the moons orbit. This notion of self-correction is similar to the oscillatory coupling modeled by the Kuramoto model (Section 4).

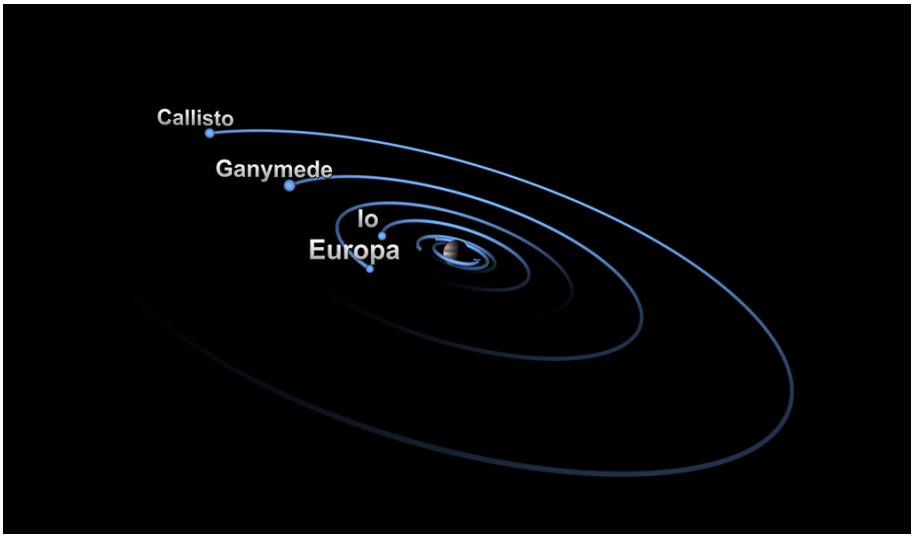

Figure 20: Jupiter's Galilean moons: Io, Europa, Ganymede, and Callisto [Kas13].

A study on another astronomical synchronization phenomenon is *Mysterious Coherence in Several-megaparsec Scales between Galaxy Rotation and Neighbor Motion* [LPS+19]. In this paper, the rotational coherence between galaxies is analyzed and experimentation is conducted to determine the distance galaxies can be from each other to still maintain rotational coherence. The paper furthers

their findings by proposing a "possible relationship between the long-term motion of a large-scale structure and the rotations of galaxies in it" [LPS+19]. Once more, parallels can be drawn between the ability of galaxies to synchronize and the ability of a system of double pendulums to synchronize under chaotic conditions.

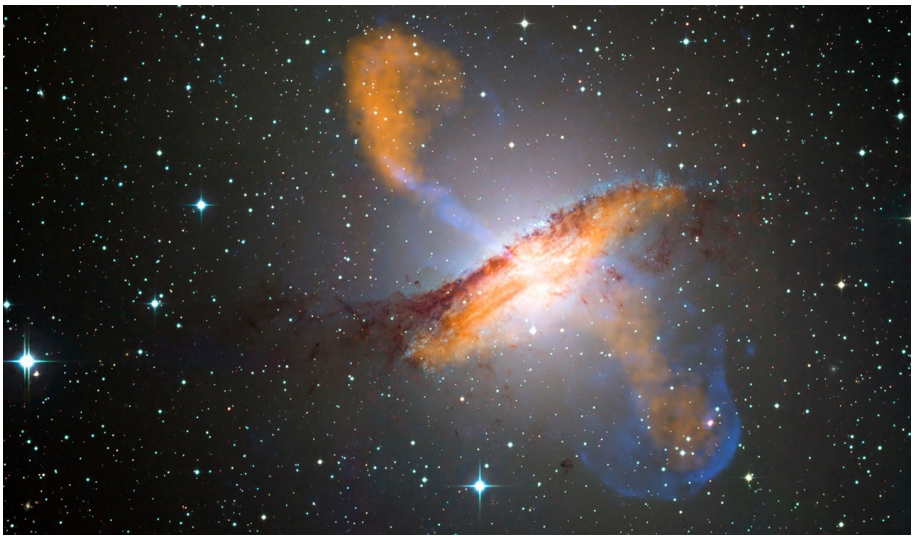

Figure 21: Centaurus A galaxy [Mag18].

An example of synchronization in chemistry is the Belousov–Zhabotinsky (BZ) reaction. In this experiment, Belousov and Zhabotinskii created a chemical reaction that changes colors in an oscillatory manner. When placed in a Petri dish, the reaction forms bubble-like shapes that slowly grow. This experiment greatly improved scientists' ability to conceptualize and simulate many biological processes such as morphogenesis.

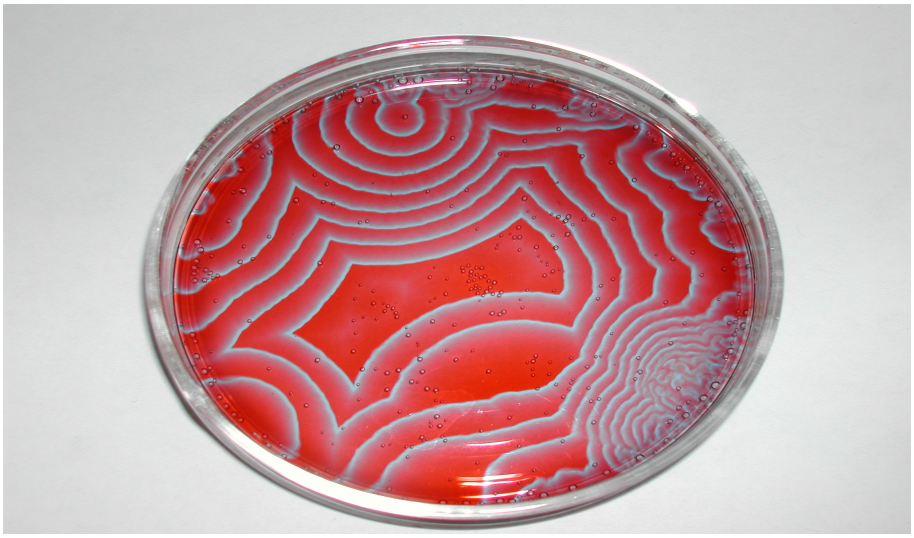

Figure 22: BZ reaction on a Petri dish [Mor04].

8 Conclusion

The ability of an orderly system to synchronize is possible through a range of initial conditions when applying the Kuramoto model. In contrast, a chaotic system, such as the double pendulum, only synchronizes under certain initial conditions such that chaos is kept at a minimum and the coupling strength has more control over the overall system. The Kuramoto model is applied throughout this paper because of its applicability for dynamic systems and parameter-driven approach to various system configurations. We see examples of this beyond the oscillatory realm where the Kuramoto model remains applicable and noise in the system can be introduced. In terms of the double pendulum, the ability of the Kuramoto model to couple N oscillators while resisting the natural communication between m_1 and m_2 for each of N oscillators is a similar phenomenon observed in nature. As is true, four real-world examples of synchronization ranging from architecture to chemistry were analyzed and parallels were drawn to the behavior of pendulums.

References

[CMMN19] Tianran Chen, Jakub Marecek, Dhagash Mehta, and Matthew Niemerg. Three formulations of the kuramoto model as a system of polynomial equations, 2019.

[GCR14] Shamik Gupta, Alessandro Campa, and Stefano Ruffo. Kuramoto model of synchronization: equilibrium and nonequilibrium aspects. *Journal of Statistical Mechanics: Theory and Experiment*, 2014(8):R08001, aug 2014.

[GHW17] Barbara Gentz, Seung-Yeal Ha, and Christian Weisel. Synchronization of the kuramoto model under noise. 2017.

[Gus21] Alexander Gustafsson. *Butterfly-effect simulation using 501 double pendulums [1440p].* https://www.youtube.com/watch?v=k3TaCGmJZ9I, Apr 2021.

[Hun07] J. D. Hunter. Matplotlib: A 2d graphics environment. *Computing in Science & Engineering*, 9(3):90–95, 2007.

[Jab08] JabberWok. *File:double-pendulum.svg.* https://commons.wikimedia.org/wiki/File:Double-Pendulum.svg, Jun 2008.

[Kas13] Alex Kasprak. *Jupiter's Many Moons.* https://svs.gsfc.nasa.gov/11173, Jan 2013.

[LPS+19] Joon Hyeop Lee, Mina Pak, Hyunmi Song, Hye-Ran Lee, Suk Kim, and Hyunjin Jeong. *Mysterious coherence in several-megaparsec scales between galaxy rotation and neighbor motion. The Astrophysical Journal*, 884(2):104, 2019.

[LRP07] Richard Watkins LRPS. *Millennium Bridge.* http://www.flickr.com/photos/65983156@N03/6135568381/, 2007.

[Mag18] Science Magazine. *These synchronized galaxies are upending what we know about the universe.* http://www.youtube.com/watch?v=y8Q5IDIkUzY, Feb 2018.

[Mor04] Stephen Morris. Belousov zhabotinsky reaction. "http://www.flickr.com/photos/nonlin/3572095252", 2004.

[MTP+21] David Mersing, Shannyn A Tyler, Benjamas Ponboonjaroenchai, Mark R Tinsley, and Kenneth Showalter. *Novel modes of synchronization in star networks of coupled chemical oscillators. Chaos: An Interdisciplinary Journal of Nonlinear Science*, 31(9):093127, 2021.

[Oli21] Travis Oliphant. *Scipy.integrate.odeint.* https://docs.scipy.org/doc/scipy//reference/generated/scipy.integrate.odeint.html, 2021.

[PRONA16] Jonatan Peña Ramirez, Luis Alberto Olvera, Henk Nijmeijer, and Joaquin Alvarez. The sympathy of two pendulum clocks: beyond huygens' observations. *Scientific reports*, 6(1):1–16, 2016.

[RPJK16] Francisco A. Rodrigues, Thomas K. DM. Peron, Peng Ji, and Jürgen Kurths. *The Kuramoto model in complex networks. Physics Reports*, 610:1–98, 2016. The Kuramoto model in complex networks.

[Sha22] Kaival Shah. The Synchronization of Single and Double Pendulums With the Kuramoto Model. https://drive.google.com/drive/folders/1D67BKB1MMp00SpPsuPoi3uWA1kLbMxXT?usp=sharing, 2022.

[Str04] Steven Strogatz. *Sync: The emerging science of spontaneous order*. Penguin UK, 2004.

[sys18] *Jupiter's Moons*. http://www.system-sounds.com/jupiters-moons/, Apr 2018.

[VGO+20] Pauli Virtanen, Ralf Gommers, Travis E. Oliphant, Matt Haberland, Tyler Reddy, David Cournapeau, Evgeni Burovski, Pearu Peterson, Warren Weckesser, Jonathan Bright, and et al. *SciPy 1.0: Fundamental algorithms for scientific computing in python*. *Nature Methods*, 17(3):261–272, 2020.

[VHFMP21] John Vandermeer, Zachary Hajian-Forooshani, Nicholas Medina, and Ivette Perfecto. *New forms of structure in ecosystems revealed with the Kuramoto model*. *Royal Society Open Science*, 8(3), 2021.

[WG22] Gerd Wagner and Matthew W. Guthrie. Demystifying the lagrangian of classical mechanics, 2022.

[Yes20] Boran Yesilyurt. Equations of motion formulation of a pendulum containing n-point masses, 2020.